Exceptional endocranium and middle ear of Stanocephalosaurus (Temnospondyli: Capitosauria) from the Triassic of Algeria revealed by micro-CT scan, with new functional interpretations of the hearing system

Thomas Arbez, Anissa Dahoumane, J.-Sébastien Steyer

Braincase and middle-ear of *Stanocephalosaurus* nov. sp. (Temnospondyli: Capitosauria) from the Triassic of Algeria studied by micro-CT scan, with new interpretation of hearing system functioning

Thomas Arbez[1*], Anissa Dahoumane[2], J.-Sébastien Steyer[1]

[1] Centre de Recherches en Paléobiodiversité et Paléoenvironnements (UMR 7207), Sorbonne Universités, CNRS-MNHN- UPMC-EPHE, Muséum national d'Histoire naturelle, CP 38, 8 rue Buffon, 75005 Paris, France

[2] Laboratoire Géodynamique des Bassins Sédifmentaires et des Orogènes, FSTGAT-Université des Sciences et de la Technologie Houari Boumedienne, BP 32 El Alia, Bab Ezzouar, Algier, Algeria

*tarbez@edu.mnhn.fr

ADDITIONAL KEYWORDS: amphibian - artery - braincase - endocranium - otic - paleobiology - stapes - tetrapod – temnospondyl - tomography

Abstract

Temnospondyls form a large clade of extinct non-amniotic tetrapods. Although their external cranial anatomy is relatively well known, their endocranium (i.e. internal structures of the skull) remains poorly known due to the lack of well-preserved material with conservation of the original anatomic volume. Internal structures are generally crushed under the skull roof due to the frequent flattening of skulls during fossilisation. Yet this region is of great paleobiological interest with respect to the hearing, nervous and vascular systems. In addition, endocranial characters have already been shown to be phylogenetically very informative in various vertebrate groups (e.g. mammals, dinosaurs). An exquisite skull belonging to *Stanocephalosaurus amenasensis* from the Lower-Middle Triassic of the Zarzaïtine Series (Algeria) has been investigated by X-ray micro-CT (computed-tomography) scan. The resulting 3-D reconstruction of this unique specimen reveals highly detailed anatomy of the endocranial region, which is described herein. In addition, both columellar cavity and stapes morphologies lead to a new functional hypothesis for the stapes as part of an underwater hearing system. This endocranium description increases our knowledge of temnospondyl paleobiology and endocranial structure variability. The hearing system postulated in *Stanocephalosaurus amenasensis* provides an evolutionary scenario which is also compared with that of extant anurans.

Introduction

Temnospondyls form a large clade of extinct non-amniotic tetrapods. Among them, capitosaurs were very widespread and diversified during the Triassic. Most of them had an amphibious to aquatic lifestyle and occupied various ecosystems such as rivers, lakes, swamps, and shores (e.g. Schoch & Milner, 2000; Warren, 2000; Fortuny et al. 2011). As non-amniotic tetrapods (i.e. amphibians), they are often compared with lissamphibians, but they contrast greatly with these due to their large size range – reaching an average body length of 1-2 meters with species exceeding 5 meters – and their massive skulls (e.g. Schoch, 1999a; Steyer & Damiani, 2005).

These great morphological contrasts make comparisons with extant amphibians difficult. Consequently, relationships between lissamphibians and different groups of fossil amphibians (including temnospondyls) are still debated (e.g. Laurin & Reisz, 1997; Ruta & Coates, 2007; Carroll, 2007). Most of the characters used in these phylogenies are extracted from the skull roof, the palate and/or the postcranial skeleton: few endocranial characters have been taken into account so far. Yet in other tetrapods (e.g. mammals, dinosaurs), endocranial characters have been shown to be phylogenetically very informative (e.g. Macrini, Rowe & Archer, 2006; Balanoff, 2011).

Endocranial structures of temnospondyls are only known from a few exceptionally well-preserved specimens belonging to *Edops craigi* Romer, 1936 (Romer & Witter, 1942); *Eryops megacephalus* Cope, 1877 (Sawin, 1941); *Dvinosaurus egregius* Shishkin, 1968 (Shishkin, 1973), *Benthosuchus sushkini* (Efremov, 1929) (Bystrow & Efremov, 1940); *Lyrocephaliscus euri* (Wiman, 1914) (Säve-Söderbergh, 1936; Mazin & Janvier, 1985); *Mastodonsaurus giganteus* (Jaeger, 1828) (Schoch, 1999a); and *Paracyclotosaurus davidi* Watson, 1958. Recently, X-ray microtomography scans of skulls belonging to *Dendrerpeton acadianum* Owen, 1853 (Robinson, Ahlberg & Koentges, 2005) *Doleserpeton annectens* Bolt, 1969

(Sigurdsen, 2008) and *Gerrothorax pulcherrimus* (Fraas, 1913) (Witzmann et al., 2011) have contributed to our knowledge. Nevertheless, the endocranium is still relatively poorly known in temnospondyls. The principal reason is linked with the preservation of the specimens, which are ironically compared with “road-killed amphibians” (A. R. Milner, pers. comm. 1999): their skulls are indeed frequently dorsoventrally very compressed, and their endocranial structures completely crushed.

An exceptionally well-preserved skull of the capitosaurian *Stanocephalosaurus*, recently found in 3-D in the Triassic of Algeria (Nedjari et al. 2010), has been used for cranial exploration: specimen ZAR05 (collections of the University of Alger) has been analysed by X-ray micro-CT scan AST-RX at MNHN, Paris. Its complete endocranial description is given here based on the resulting highly detailed 3-D computer-based reconstruction, and leads to new morphological observations and interpretations.

Another point of interest highlighted by endocranial investigations concerns the paleobiology of temnospondyls associated with the hearing, nervous and/or arterial systems. In particular, the hearing system of temnospondyls remains ambiguous: indeed, the stapes is often considered as a middle ear bone, i.e. a part of a tympanic ear close to the anuran condition and linked with acoustic function (e.g. Bold & Lombard, 1985; Schoch, 2000). However this bone is sutured with the parasphenoid in several taxa such as *Eryops megacephalus* (Sawin, 1941), *Dissorophus multicinctus* Cope, 1895 (DeMar, 1968), *Lyrocephaliscus euri* (Mazin & Janvier, 1983), *Tersomius texensis* Case, 1910 (Carroll, 1964) or *Stanocephalosaurus* studied here. This peculiar condition questions the traditional acoustic function attributed to the stapes, which could also play a role in support of the spiracular canal (Warren & Schroeder, 1995). The highly detailed anatomy of the columellar cavity and stapes of *Stanocephalosaurus*

studied here leads to a new hypothesis of the stapes function, as part of a hearing system adapted to underwater sound perception.

Material and Methods

Specimen ZAR05

The studied taxon is the capitosaurian temnospondyl *Stanocephalosaurus amenasensis*. (Dahoumane et al., 2016) from the Lower-Middle Triassic of the Zarzaïtine Series, Illizi Basin, Southeastern Algeria. The analysis is based on an exquisite skull (specimen ZAR05 of the collections of the Faculté des Sciences de la Terre, de Géographie et de l'Aménagement du Territoire, Alger, Algeria; Fig. 1) collected in a Lagerstätte (Nedjari et al., 2010; Aït-Ouali et al., 2011) and preserved in 3-D. This skull is about 23.5 cm in length (only the tip of the snout is missing) and its dorsal surface ornamented, as in adult temnospondyls (e.g. Steyer, 2000). The orbits are proportionally small and dorsally exposed. The snout (or preorbital region) is elongated and naturally flattened, as in all capitosaurians. The postorbital region is comparatively shorter but much deeper, with large and semi-closed otic notches, a character found in the genus *Stanocephalosaurus*. We refer to Dahoumane et al. (2016) for a more complete description of this Algerian taxon. The exceptional preservation of this specimen ZAR05 allows its endocranial region to be studied: the specimen indeed does not show any post-mortem deformation or bone displacement; as exemplified by its stapes, which are both *in-situ*, i.e. sub-vertically preserved in their respective otic notches (Fig. 2A, B).

X-ray micro-CT scan information

The postorbital region of ZAR05 was scanned at the AST-RX facility of the MNHN (Paris) using the microfocus beam 240 kV of the CT-scan with the following parameters: voltage, 175 kV; current, 420 μA; voxel size, 0.06539 mm; slices resolution, 1790 x 2024 pixels. In

total, 2018 virtual slices showing internal structures were reconstructed using GE Sensing & Inspection Technologies Phoenix|x-ray datos|x rec. These slices were imported in the 3-D reconstruction software Mimics 17.0 (Materialise, Leuven, Belgium). To render the data more manageable, the slices were previously cropped to 1714 x 1064 pixels in order to remove the maximum of empty space. To decrease the data size, the resolution was also previously reduced by two, giving 1009 slices with a resolution of 857 x 532 pixels and a voxel of 0.13078 mm. The 3-D model was produced by segmentation using the "thresholding" function (with greyscale from 15000-18000 to 50288 depending on the anatomical feature of interest on each slice). The 3-D model was produced with the same voxel resolution and with a "Smooth Factor" of 1.0 and five iterations, in order to reduce surface irregularities due to manual segmentation. In order to render some very small (parasphenoid and exoccipital) canals clearly visible on the 3-D PDFs, their diameter has been artificially increased by few pixels. Data produced by segmentation were exported in the software 3matic 9.0 for PDF 3-D creation available in Supplementary Information. (Maximum quality data are unusable on a personal computer. If you are interested in a 3-D model with these data, please ask the corresponding author).

Systematic palaeontology

TEMNOSPONDYLI Zittel, 1887-1890

STEREOSPONDYLI Zittel, 1887-1890 (sensu Yates and Warren, 2000)

CAPITOSAUROIDEA Watson, 1919 (sensu Schoch and Milner, 2000 = "MASTODONSAUROIDEA" sensu Damiani, 2001)

PARACYCLOTOSAURIDAE Ochev, 1966

STANOCEPHALOSAURUS Brown, 1933

STANOCEPHALOSAURUS AMENASENSIS Dahoumane, Nedjari, Aït Ouali, Taquet, Vacant and Steyer, 2016

Abbreviations

a cl (pal ar?)	anterior canalicule (palatine artery?)
a ext	anterior extension of the processus lamellosus
a f ps (pal ar?)	anterior foramen of the parasphenoid (palatine artery?)
a f pt (pal n?)	anterior foramen of the pterygoid (palatine nerve?)
a w	anterior wall
am cav	anteromedial cavity
b op (sub fos)	basal opening (substapedial fossa)
bo	basioccipital (remains)
cr a smc	crista for the anterior semicircular canal
cr latsph	crista laterosphenoidales
cr mus	crista muscularis
cr o o	lateral opening of the crista obliqua
cr par	crista parotica
cr pt	crista parapterygoidea
dl cl (art?)	dorsolateral canalicule (arteriole?)
dl cl f (art?)	foramen of the dorsolateral canalicule (art?)
d λ	dorsal branch of the delta groove
epi	epipterygoid
exo	exoccipital
fen ov	fenestra ovalis
fm	foramen magnum
fo	fovea ovalis
fos I (l sc c?)	fossa I (lateral semi-circular canal?)
fos II (a sc c?)	fossa II (anterior semi-circular canal?)
fp	footplate
fr	frontal
gr	groove
ins pr	insertion process of the stapes on the parasphenoid
ju	jugal
l cd (XII?)	lateral conduct (hypoglossal nerve?)
l f (XII?)	lateral foramen (hypoglossal nerve?)
l op (jug?)	lateral opening (jugular?)

	m λ	medial branch of the delta groove
	mar	margin of the conical recess
	mus po	muscular pocket
	no	notch
	opi	opisthotic
	orn	ornamentation
	p cd (vas?)	posterior conduct (vascular?)
	p cr	posterior crest
	p f (vas?)	posterior foramen (vascular conduct?)
	pa	parietal
	pc (aci)	principal canal (arteria carotis interna)
	pc a f (aci)	anterior foramen of the principal canal (arteria carotis interna)
	pc p f (aci)	posterior foramen of the principal canal (arteria carotis interna)
	pf	postfrontal
	por	postorbital
	pp	postparietal
	pro	prootic
	prot	protuberance
	ps	parasphenoid
	pt	pterygoid
	ptf	post-temporal fossa
	q	quadrate
	r c	conical recess
	rug	rugose area
	s exo	suture with the exoccipital
	s pp	suture with the postparietal
	s ps	suture with the parasphenoid
	s pt	suture with pterygoid
	s q	suture with the quadrate
	s t	suture with the tabular
	spt	supratemporal
	sq	squamosal
	st f	stapedial foramen
	stp	stapes
	t	tabular
	v λ	ventral branch of the delta groove
	vl cl (art?)	ventrolateral canalicule (arteriole?)

Description

The CT-scan and the exceptional preservation of the specimen allow each bone of the braincase and middle-ear regions to be described precisely (Fig. 2A, B).

Parasphenoid (Figs. 3A-F, 4)

The two typical elements of this bone, i.e. the cultriform process anteriorly and the basal plate posteriorly, are distinctly visible in 3-D.

The cultriform process connects the anterior part of the basal plate with the vomers and medially forms the interpterygoid vacuities. Dorsally, it bears the anterior part of the brain. This cultriform process measures about 130 mm in length (26 mm for the modelled part) and 4-16 mm in width. It is thin, elongated and relatively straight. Its slender morphology contrasts with the very robust cultriform process of *Dutuitosaurus ouazzoui* (Dutuit, 1976). Its lateral margins are slightly concave, and its dorsal surface is laterally bordered by two crests, the ‘cristae laterosphenoidales’ sensu Schoch (1999a: 50). These crests border the brain and/or the sphenethmoid, giving the bony element a peculiar transversal “gutter-like” cross-section. They are anteriorly thinner and rise higher gradually. The ventral side of the cultriform process is convex over almost all its length.

The basal plate of the parasphenoid, or parasphenoid plate, is 42 mm in length and 47 mm in width, and octagonal in shape. It is 3 mm thick at the centre, with an increasing thickness peripherally, especially toward the pterygoids with a maximum thickness of 7 mm (16 mm at the level of the cristae parapterygoideae). In proportions, this basal plate is very different to that of the other capitosaur *Paracyclotosaurus davidi* which is about twice as long as wide (Watson, 1958). It bears the posterior part of the brain, the basisphenoid cartilage and the otic capsules. Posteriorly, it is firmly connected to the exoccipital and laterally forms the

basicranial articulation with the pterygoid (Fig. 2B). The basal plate of *Stanocephalosaurus amenasensis* is fully sutured with the pterygoid, a typical stereospondyl character (e.g. Yates & Warren, 2000). This renders the pterygoid-parasphenoid association stable rather than mobile. This octagonal basal plate has seven sides (the eighth corresponds to the insertion area with the cultriform process): two anterior, two anterolateral, two posterolateral, and a posterior one (Fig. 3A). The anterior sides form the posterior limit of the interpterygoid vacuities and the beginning of the cultriform process. The anterolateral sides form the suture with the basipterygoid branch of the pterygoid, while the posterolateral sides form the suture with the subtympanic process and the occipital condyles of the exoccipital (Fig. 3 A-D). At least, the posterior side of the basal plate forms an elongated surface or "projection", which is slightly slopping posteriorly. This projection ventrally separates the occipitals condyles and ends with a small posterior border. Paradoxically, this morphology resembles that of the metoposaur *Metoposaurus diagnosticus* (von Meyer, 1842) (Sulej, 2007: fig. 2) but is different from that of the close relative *Mastodonsaurus giganteus* where this posterior projection is absent (Schoch, 1999a). In *Stanocephalosaurus amenasensis*, the basal plate is firmly connected to the exoccipital with which it shares an interdigitated suture (i.e. a firm suture with numerous small grooves and extensions), one of the longest of the endocranium (Fig. 3F). The ventral surface of this basal plate is concave and has a slight ornamentation composed of small alveoli gradually radiating into elongate but still shallow ridges and grooves (Fig. 3B). This typical "honeycomb" ornamentation is much marked on the pterygoids and, above all, on the skull roof bones (Fig. 1, 2A). The ventral surface of the posterior projection of the parasphenoid plate bears a pair of 'muscular pockets' sensu Watson (1962: 229), which correspond to ovoid and posteriorly open small depressions for the insertion of the hypaxial muscles (Fig. 3B). These pockets are anteriorly bordered by a well-defined curvilinear crest, which is especially strong in its medial part, called the 'crista

muscularis' sensu Watson (1962: 229). Delimited by these pockets, the parasphenoid has a posteriorly oriented tip. The dorsal surface of the parasphenoid plate forms the floor of the posterior region of the brain on which it would lie (Fig. 3A). This surface is marked by slight crests and transversal depressions. Laterally, at the level of the pterygoid suture, the dorsal surface also bears a pair of elevated and half-cone structures named the 'cristae parapterygoideae' sensu Bystrow & Efremow (1940: fig. 9A) (= parafenestral crista sensu Säve-Söderbergh, 1936: 21). The lateral extremity of these cristae is oriented toward the proximal end of the stapes. The right crista contacts the 'insertion process of the stapes on the parasphenoid' ('processus d'insertion du stapes sur le parasphénoïde' Mazin & Janvier, 1983: 21) of the right stapes (here abbreviated by "insertion process"). It is defined as a small triangular process linking the stapes to the cristae parapterygoideae. The margins between these cristae and the base of the cultriform process form on each side the medial part of a sub-conical concavity. This rounded depression, relatively deep and located on both parasphenoid and pterygoid, is called the 'conical recess' sensu Säve Söderbergh (1936: 18). These margins follow the cristae laterosphenoidales of the cultriform process anteriorly, while posterolaterally they follow the anterior base of the cristae parapterygoideae and continue on the pterygoids. The anterior part of the conical recess is located under the basal part of the epipterygoid.

Dorsally, two oval and relatively large foramens (4 x 2 mm for the left one; 2 x 1 mm for the right one) pierce the anteromedial part of the basal plate - the left one is more anterior than the right one (Fig. 3). They turn internally into curved and large canals (1.3 mm in average diameter), called here the principal canals. These canals cross the basal plate and emerge posteriorly below the cristae parapterygoideae. They diverge into smaller, secondary canalicules, which are not symmetrical: the left anterior canalicules, relatively straight, are dichotomic, whereas the right ones are totally separated. These anterior canalicules emerge on

the anterior margin of the basal plate, except for the medial right anterior one, which emerges along the cultriform process. Dorsolateral canalicules also emerge from the principal canals: the right ones are partly subdivided peripherally, whereas the left ones are totally subdivided. These canalicules emerge at the level of the conical recess. At least, two ventrolateral canalicules emerge from the left principal canal and emerge ventrally, on the posterolateral left side of the parasphenoid plate. No similar canalicule or foramen is visible on the right side.

***Epipterygoid* (Fig. 5A-F)**

This bone lies on the pterygoid and delimits, with the sphenethmoid, the lateral side of the braincase. It is here composed of three processes emerging from the 'vertical lamina' ('lamelle verticale' sensu Dutuit, 1976: 84); the 'processus dorsalis', the 'processus posterior' and the 'processus basalis' sensu Schoch (1999a: 62). This epipterygoid composed of three processes is very different from that of *Benthosuchus sushkini*, which simply has a vertical lamina, or from that of *Mastodonsaurus giganteus*, which bears six distinct processes (Schoch, 1999a).

The vertical lamina is sub-rectangular with anterior and posterior smooth surfaces (Fig. 5A, B). The anterior surface is convex, whereas the posterior one is concave. The ventral surface of this lamina is pierced by about 10 submillimetric foramens (Fig. 5F). Their exact number, position and size vary slightly between the left and right epipterygoid, which suggests nutritive foramens. Ventrally, a curved groove separates this lamina from the processus basalis, rendering the epipterygoid composite. This pattern is very different from that of *Mastodonsaurus giganteus*, in which the epipterygoid has a single ventral 'footplate' sensu Schoch (1999a: 62).

The processus dorsalis is a bony blade, narrow at its base but which gradually widens dorsally (Fig. 5A, B), as in *Paracyclotosaurus davidi* (Watson, 1958: fig. 4). Its orientation in the endocranium is transversal (Fig. 2B), as in *Metoposaurus diagnosticus* (Sulej, 2007: fig. 2). Its anterior and posterior sides are smooth, the anterior side being slightly concave and the posterior one relatively flat. Its dorsal side is also slightly concave but rugose, suggesting a cartilaginous zone (Fig. 5C).

The processus posterior is a bony blade of sub-rectangular cross-section (Fig. 5A, B). Its orientation is the same as that of the vertical lamina. It is shorter and wider than the processus dorsalis. The anterior and posterior surfaces of the processus posterior are smooth. Its contact with the pterygoid is not continuous, maybe due to a cartilaginous prolongation.

The processus basalis is the posterior extension of the vertical lamina (Fig. 5B). It has a hook shape and an oblique orientation. It is aligned laterally with the anterior notch of the pterygoid (see below). Its ventral surface bears about 20 submillimetric foramens, *a priori* nutritive (Fig. 5F). The medial extremity of the processus basalis is concave (Fig. 5C), suggesting a cartilaginous zone, as in *Mastodonsaurus giganteus*. Its ventral surface partially contacts the pterygoid, as in *Dutuitosaurus ouazzoui*. This partial contact also suggests a cartilaginous area (Dutuit, 1976).

Pterygoid **(Fig. 6A-F)**

This quadri-radiated bone is composed of the palatine ramus (partly reconstructed here), the basipterygoid ramus, the quadrate ramus and the dorsal ramus (or ‘lamina ascendens’ sensu Schoch, 1999a: 54). It is involved in the skull stability in ‘[connecting] the upper jaw with the quadrate condyles, the cheek region, the occipital condyles, and the floor of the braincase’ (Schoch, 1999a: 54).

The palatine ramus is the widest and the longest ramus of the pterygoid (83 x 26 mm; Fig. 6A, B). Located in the horizontal plan, it forms a wide and thick sheet of bone, similar to that of *Benthosuchus sushkini* (Bystrow & Efremov, 1940: fig. 5). Its anterior extremity contacts the ectopterygoid, the palatine and the jugal. Its medial edge, slightly concave, forms the posterior half of the lateral border of the interpterygoid vacuity. Its lateral edge, forming the medial border of the subtemporal window, is sigmoid: concave at the base of the ramus, it becomes convex at mid-length due to a lateral enlargement called the 'transverse flange' (sensu Damiani, 2001: 388). Paradoxically, it resembles the palatine rami found in *Benthosuchus sushkini* and *Metoposaurus diagnosticus*, rather than in its close relatives *Mastodonsaurus giganteus* and *Paracyclotosaurus davidi* where this structure is straight. In *Stanocephalosaurus amenasensis*, the dorsal surface of the palatine ramus is rather smooth but has a slight groove running laterally along its transverse flange and delimiting the quadrate ramus from the lamina ascendens (Fig. 6C, F). This groove is similar to that observed in *Dutuitosaurus ouazzoui* and *Lyrocephaliscus euri* (T.A., pers. obs. on respectively MNHN F.AZA 341-1 and MNHN F.SVT 520). In *Stanocephalosaurus amenasensis*, the ventral surface of the palatine ramus is ornamented over all its length with the "honeycomb" pattern (Fig. 6B), excepted on its medial edge.

The basipterygoid ramus is very short compared to the others rami (Fig. 6A, B), as in *Benthosuchus sushkini*. This suggests that the basipterygoid articulation is not functional. This pattern differs from *Edops craigi*, which has a functional basipterygoid articulation (Schoch, 1999b). This ramus shares an interdigitated and long suture (about 25% of the pterygoid length) with the parasphenoid, as in *Paracyclotosaurus davidi* and *Benthosuchus sushkini*. In *Stanocephalosaurus amenasensis*, the anterior edge of this ramus also bears a triangular extension, which extends medially and contacts the anterior edge of the parasphenoid plate. On the left pterygoid, the anterior edge of this extension bears a foramen (Fig. 6C). An oval

depression is visible on the anterodorsal portion of this branch and on the anteroventral part of the lamina ascendens (Fig. 6A, B, E). This depression continues on the parasphenoid and forms the conical recess (see above). This pattern is close to that observed in *Mastodonsaurus giganteus* but differs in many other temnospondyls in which the conical recess is located either more medially (e.g. *Dvinosaurus primus* Amalitskii, 1921) or anteriorly to the lamina ascendens (e.g. *Benthosuchus sushkini*). The posterolateral extremity of the basipterygoid branch partly bears a wide opening, jointly formed with both parasphenoid and exoccipital. This opening leads to the endocranial cavity dorsally, at the level of the columellar cavity, and to the buccal cavity ventrally.

The quadrate ramus of the pterygoid is sub-vertical and with a medially inclined ventral margin (about 15-20°; Fig. 6A, B). It contacts the quadrate posteriorly in an elongate and interdigitated suture, which is also shared with the lamina ascendens. The exact posterior limit of the quadrate ramus is difficult to delimit due to a scanning artefact. The lateral edge of this ramus is concave and forms the posteromedial part of the sub-temporal window, whereas its medial edge is convex. In ventral view, this ramus is posterolaterally inclined about 45°, as in *Benthosuchus sushkini*. This angle is more acute than that measured in *Mastodonsaurus giganteus*.

The dorsal ramus or lamina ascendens is slender and sub-vertical, and laterally delimits the columellar cavity (Fig. 5A). Its lateral and medial surfaces are smooth. It is transversally orientated with its anterior extremity pointing medially. This anterior extremity contacts the basipterygoid branch on its posterior half and bears a slight concavity corresponding to the anterior part of the conical recess. The dorsal half of this anteromedial margin contacts the prootic, while the ventral half contacts the lateral margin of both the processus posterior and the vertical lamina of the epipterygoid (Fig. 2B). At mid-height, this margin also has a

peculiar semi-circular notch (Fig. 6A, E). The notch follows the posterodorsal extension of the processus basalis of the epipterygoid and leads to the columellar cavity. This notch is named ‘fovea ovalis’ by Bystrow & Efremow (1940). The lamina ascendens dorsally contacts the lamina descendens of the squamosal – ‘the counterpart of the lamina ascendens, formed by the squamosal, and in capitosaurs usually closing the occipital face of the cheek’ (Schoch, 1999a: 164) - and has a sub-vertical and medial extension running along the lamina ascendens. This extension, named ‘crista obliqua’ by Bystrow & Efremow (1940: fig. 5), begins anteriorly at the inflexion point of the anterior curve of the lamina ascendens and is dorsally oriented (Fig. 6A, E). It forms a canal dorsally leading laterally to the lamina descendens of the squamosal. The posteromedial surface of the crista obliqua is slightly concave and rugose (Fig. 6D), as in *Mastodonsaurus giganteus*. In *Stanocephalosaurus amenasensis*, the crista obliqua is well developed: this is considered to be an autapomorphy of Capitosauroidea by Damiani (2001).

***Otic capsule* (Figs. 7A-F, 8A-F)**

The otic capsule is not commonly observed in temnospondyls. In *Stanocephalosaurus amenasensis*, it is weakly ossified, with the prootic and the opisthotic totally separated, as is the case in *Dendrerpeton acadianum* or *Doleserpeton annectens* but not in *Edops craigi* or *Eryops megacephalus* in which the prootic and the opisthotic are in contact. This separation of the prootic and the opisthotic suggests a cartilaginous zone between the bones, a hypothesis supported by the inner spongious structure of these elements. The otic capsule of *Stanocephalosaurus amenasensis* is also in contact with the exoccipital posteriorly, with the pterygoid laterally, and is ventrally close to the dorsal surface of the proximal part of the stapes (Fig. 2B). This otic capsule forms the dorsal edge of the fenestra ovalis, an opening bordered here by the otic capsule, the pterygoid, the parasphenoid and the exoccipital and into

which the stapes fits in natural articulation. This opening allows contact between the stapes and the perilymphatic cistern, a vesicle of the inner ear. In some species, the pterygoid borders the basioccipital (e.g. *Eryops megacephalus*) but not the fenestra ovalis (e.g. *Doleserpeton annectens*, *Trimerorachis insignis* Cope, 1878). The outline of the fenestra ovalis is not well delimited because it corresponds to a space between these different structures, as in *Mastodonsaurus giganteus* but not in *Eryops megacephalus* where the fenestra ovalis has a simple circular outline (Schoch, 1999b: fig.4).

The prootic has an anteromedial and a posterolateral extension, separated by a groove (Fig. 7C, D). The ventral edge of the prootic forms the anterodorsal border of the fenestra ovalis. The anterior portion of the prootic is large and smooth, as in *Dendrerpeton acadianum* (Robinson et al., 2005). It forms a slightly concave anterior wall (Fig. 7A) pierced by 5 to 10 sub-millimetric foramens. As their number and position vary depending on the left or right prootic, these foramens seem nutritive, not related to the nervous system. The anterior wall of the right prootic has a small notch at mid-height on its medial border (Fig. 7A). A wide, deep and straight fossa also runs on the prootic, from its anterolateral edge to its dorsal region (Fig. 7C, D). The anterior part of this fossa receives the dorsal half of the pterygoid anteromedial margin, while its posterior part corresponds to the ‘post-temporal fossa’ described in *Dendrerpeton acadianum* by Robinson et al. (2005: fig. 8) and named ‘fossa bridgei’ by Säve-Söderbergh in *Lyrocephaliscus euri* (1936: fig. 11). *Edops craigi* and *Lyrocephaliscus euri* have a totally ossified otic capsule with a fossa running all along its dorsal surface. The post-temporal fossa described here (and that seen in *Dendrerpeton acadianum*) would therefore be the anterior part of a larger fossa which existed when the animal lived. In dorsal view, this fossa delimits two parts of the prootic (Fig. 7D). The posterolateral one, with a semi-circular cross-section, is similar to *Dendrerpeton acadianum*. It corresponds to the ‘crista parotica’ sensu Robinson et al. (2005), a protrusion housing the lateral semi-circular

canal (Fig. 7A-C). In *Stanocephalosaurus amenasensis*, the medial part of the prootic has a sub-oval cross-section and may house the anterior semi-circular canal (Fig. 7A, D), as in *Doleserpeton annectens* (Sigurdsen, 2008: fig. 6). In posterior view, the surface of the prootic is irregular and rugose, suggesting a cartilaginous area. This surface has a fossa parallel to the crista parotica (which could house the lateral semi-circular canal according to Robinson et al., 2005) and a fossa medial to the crista parotica, which could house the anterior semi-circular canal as suggested in *Dendrerpeton acadianum* (Robinson et al., 2005: fig. 9) and *Doleserpeton annectens* (Sigurdsen, 2008: fig. 6).

The opisthotic is ovoid and has an anteromedial cavity (Fig. 8A, D). It differs from the opisthotic of *Doleserpeton annectens*, massive and bearing three extensions (Sigurdsen, 2008: fig. 7). Its anterior surface is irregular and rugose, suggesting a cartilaginous area (Fig. 8A). Its posterior and ventral parts, ossified, are fused with the exoccipital at the level of the processus paroticus and of the anterior surface of the columna verticalis. The anterolateral edge of the opisthotic forms the posterior border of the fenestra ovalis. Numerous foramens, a priori nutritive, pierce the anteroventral surface of the opisthotics (20-30 on the right one, more than 50 on the left one). The anteromedial cavity of the opisthotic, in anterior view (Fig. 8A), would correspond to the junction between the lateral and posterior canals, as in *Doleserpeton annectens* (Sigurdsen, 2008, fig. 6). The posterior surface of the opisthotic is not visible in occipital view due to its contact with the columna verticalis and the processus paroticus of the exoccipital. In posterior view, this surface has a crest, slightly curved, which extends from the medial to the lateral edge of the opisthotic (Fig. 8B). This crest is clearly distinct on the right opisthotic but very low on the left one. It could correspond to the ‘paroccipital process’ sensu Sigurdsen (2008: 744) seen in *Doleserpeton annectens*.

***Stapes* (Fig. 9A-F)**

The stapes of *Stanocephalosaurus amenasensis* are preserved in-situ, in the columellar cavity, which follows the lamina ascendens of the pterygoid laterally and the processus paroticus medially. As both left and right stapes have exactly the same position, they are *a priori* in living position (Fig. 2B). This columellar cavity opens dorsally toward the otic notch. The stapes is nicely preserved in 3-D: it is composed of a columellar shaft, called the 'stylus columellae', and a bifurcating proximal head with a 'Ventral Proximal Head' (VPH) and a 'Dorsal Proximal Head' (DPH) sensu Lombard & Bolt (1988).

The stylus columellae is aligned with the posterior part of the crista obliqua of the pterygoid, and ends at the level of the otic notch, more precisely at the level of the inflexion point of the concave border of the tabular.

The VPH is in the major axis of the columellar shaft, whereas the DPH is larger and bifurcates from the major axis (Fig. 9E). Each head has a rough proximal surface called 'footplate' sensu Romer & Witter (1942: 948; here Fig. 9B). This footplate, slightly concave (as in *Mastodonsaurus giganteus* or *Doleserpeton annectens*), has a spongious structure difficult to delimit precisely. In *Stanocephalosaurus amenasensis*, both stapes have a wide and sub-circular DPH and a sub-oval VPH. The VPH fits in the fenestra ovalis. A lateral extension of sub-triangular shape, only present on the right VPH (Fig. 9B), is called the insertion process (Fig. 9A-F). This process is sutured with the dorsolateral end of the right crista parapterygoidea. In *Mastodonsaurus giganteus*, it appears late in the development where it sutures the parasphenoid (Schoch, 2000). In *Stanocephalosaurus amenasensis*, the left stapes does not have this process. This suggests that specimen ZAR05 corresponds to an individual which did not completely finish its ossification. The proximal end of the dorsal surface of the VPH is nearly in contact with the posteroventral area of the prootic. The surface of the DPH is very close to the anteroventral area of the opisthotic. The anteroventral side of

the VPH has a very small foramen (≈0.6 mm), which may be the stapedial foramen based on its location (Fig. 9D, F). That of *Eryops megacephalus* is proportionally larger (2.5 mm in diameter, for a similar individual size; Sawin, 1941). The stylus columellae of the stapes is shorter and thicker than that of *Mastodonsaurus giganteus* (Schoch, 1999a: fig. 22) but not of *Edops craigi* (Romer & Witter, 1942: fig. 12). In *Stanocephalosaurus amenasensis*, it is dorsally curved, with a relatively weak slope, as in *Benthosuchus sushkini* (Bystrow & Efremow, 1940: fig. 15). The cross-section of the stylus columellae is sub-oval and slightly flattened for nearly all its length, but it is distally circular, as is the case in *Metoposaurus diagnosticus* (Sulej, 2007: fig. 1). Its distal end is slightly concave, with a rugose surface, suggesting a cartilaginous area (Fig. 9E). Yet, this shaft has a smooth surface over its entire length, as is the case in *Metoposaurus diagnosticus* where neither groove nor crest is observed. Unlike taxa such as *Lyrocephaliscus euri* with a 'retrostapedial groove' ('sillon rétrostapédial', Mazin & Janvier, 1983: fig. 6) or *Dutuitosaurus ouazzoui* with a 'transverse crest' ('crête transverse', Dutuit, 1976: fig. 29), only a small protuberance is ventrally visible on the proximal half of the columellae (Fig. 9D, F). The distal end of the columellae dorsally points toward the otic notch. It runs medially along the tabular groove and laterally along the lamina ascendens of the pterygoid.

***Exoccipital* (Figs. 10A-F, 11, 12)**

The exoccipital is formed by a robust column, the columna verticalis, which bears an articular condyle (the condylus occipitalis) and five processes named by Bystrow & Efremov (1940): the 'processus paroticus', the 'processus lamellosus', the 'processus basalis', the 'processus submedullaris' and the 'processus subtympanicus'. This bone forms the major part of the posterior region of the endocranium and has two assumed functions; to support the posterior part of the skull and to articulate it with the atlas (Piveteau, 1955). The exoccipital contacts

the tabular and postparietal dorsally (with which the sutures are interdigitated complex), the pterygoid ventrolaterally (with which the contact is limited), and the parasphenoid anteroventrally (with which the suture is interdigitated and extends until a wide foramen called here the “basal opening”; Fig. 10B, D). The foramen magnum has a ‘T-shape’ and is delimited by the exoccipitals and the postparietals (Dahoumane et al., 2016). The exoccipital includes a pair of wide and long delta-shaped grooves anteriorly (Fig. 11). Its dorsal part is formed by the descending flange of the tabular. This groove continues along both the processus paroticus and the columna verticalis, and houses the opisthotics at the anterodorsal level. At the level of the processus submedullaris, the groove splits into two branches; the medial and the lateral branch. The medial branch points posteriorly and runs along the columna verticalis and the processus submedullaris of the exoccipital. This branch ends on the dorsal surface of the posterior part of the parasphenoid, at the bottom of the foramen magnum. The lateral branch of the groove points laterally on the anterior part of the processus subtympanicus and forms the posterior side of the basal opening (see below). The upper part of this groove (before the split) has been described in “*Stanocephalosaurus*” *pronus* (Howie, 1970) as a ‘[...] space [filled] in life by the cartilaginous opisthotic’ (Howie, 1970: 215). As this groove is not named and has a delta-shape, we name it the “delta groove”.

The columna verticalis forms the main part of the exoccipital and dorsally contacts the postparietal. The columna verticalis only barely contributes to the border of the post-temporal window, unlike that of *Dutuitosaurus ouazzoui* or *Paracyclotosaurus davidi* where there is a clear contribution.

The processus submedullaris emerges medially at mid-height of the exoccipital. Its dorsal surface is reniform and slightly concave (Fig. 10B, C). Its medial surface delimits the bottom part of the lateral side of the foramen magnum.

The processus lamellosus is located above the submedullar process and medial to the columna verticalis. Its exact shape is complex and difficult to model. Its dorsal surface is subrectangular, about 2.5 longer than wide (around 8.8 x 3.6 mm for the right exoccipital), and its medial surface forms the central part of the lateral border of the foramen magnum (Fig. 10A, C). The CT-scan shows a spongious inner structure surrounded by a thin and compact cortica. This process has a very thin and short anterior extension on its anteromedial extremity (Fig. 10E, F). This is reminiscent of the processus lamellosus of *Benthosuchus sushkini* where the whole process is more extended posteriorly.

The processus paroticus is dorsolaterally projected. It is massive, with an ovoid cross-section and contacts the descending flange of the tabular (Fig. 10A). Its anterior surface, slightly concave, forms the dorsal part of the anterior groove of the exoccipital (see above). Its ventrolateral part bears a notch forming the dorsal part of an opening toward the delta-groove and the posteroventral side of the opisthotic. We call this opening the “lateral opening” (Fig. 10E, F). This processus paroticus does not contribute the sub-temporal foramen, contrary to what is seen in most temnospondyls (e.g. *Mastodonsaurus giganteus*, *Dutuitosaurus ouazzoui*).

The processus subtympanicus is anterolaterally projected and sub-triangular in posterior view (Fig. 10A). Anteriorly, it forms an interdigitated suture with the parasphenoid. Its lateral tip contacts the posterior extremity of the basipterygoid branch of the pterygoid. Its dorsal part bears a notch forming the ventral part of the lateral opening (Fig. 10B, described above). Contrary to that of *Dutuitosaurus ouazzoui*, the process of *Stanocephalosaurus amenasensis* does not extend under the stapes, due to the anterior groove of the exoccipital. This part of the groove forms the posterior surface of the basal opening, which dorsoventrally opens toward the stapes.

The occipital condyles lie in a posteromedial position and are massive, slightly wider than high (Fig. 10A, C-F). Both are well separated from each other, as in many temnospondyls (e.g. *Dutuitosaurus ouazzoui*, Dutuit, 1976: fig. 7) but not in *Trimerorachis insignis* where the condyles form a unique structure together with the basioccipital (Schoch, 1999b: fig. 1). In *Stanocephalosaurus amenasensis*, the posterior surface of the occipital condyle is rounded and granulous, and its medial part anteriorly tilted, as in *Dutuitosaurus ouazzoui* (Dutuit, 1976, fig. 3). The structure linking the bottom of the condyles anteriorly is poorly preserved (Fig. 10B-D): it could correspond to the remaining cartilage of the basioccipital, as in *Lyrocephaliscus euri* (Säve-Söderbergh, 1936: fig. 7).

Three small foramens are visible on the surface of the exoccipital: they pierce the bone and form conducts (Fig. 12). Two conducts, lateral to the exoccipital condyles, lead to the foramen magnum, above the processus submedullaris. A third conduct, posteriorly oriented and located at the bottom of the processus paroticus, leads to the posterior surface of the opisthotic. Two larger openings do not form conducts: the lateral opening, at the base of the processus paroticus, opens anteriorly near the ventrolateral part of the opisthotic; and the basal opening, at the lateral extremity of the processus subtympanicus, opens toward the basipterygoid branch of the pterygoid and the parasphenoid plate. This opening leads approximately under the ventral part of the stapes.

Discussion

Interpretations of foramens and conducts

Several foramens and conducts have been reconstructed and described above for various bones of the braincase and middle ear. They correspond to interesting characters associated with the vascular and/or nervous system. As these vascular and nervous systems have never been preserved so far as soft tissues in temnospondyls, the identification of these foramina

and conducts is based on actualistic comparisons with lissamphibians, whatever the “urodel model” (Bystrow & Efremow, 1940; Shishkin, 1973) or the “anuran model” (Säve-Söderbergh, 1936). Consequently, the same foramen is often associated with different vascular or nervous structures depending on the author(s). Here, the identification of the foramens and conducts, and their associations with a vascular and/or a nervous structure, are hypothesized only in cases of bibliographic consensus: this also allows them to be identified according to their 3-D inner reconstruction.

The parasphenoid of *Stanocephalosaurus amenasensis* is crossed by two “principal” conducts (Fig. 4), which are also visible in *Benthosuchus sushkini* (Bystrow & Efremov, 1940), *Lyrocephaliscus euri* (Mazin & Janvier, 1983), *Edops craigi* (Romer & Witter, 1942), *Eryops megacephalus* (Sawin, 1941) or *Dvinosaurus primus* (Shishkin, 1968): they are consensually assigned to the arteria carotis internae, a ramification of the arteria carotis communis observed in numerous species of *Rana* (Gaupp, 1899) and *Salamandra* (Francis, 1934). Consequently, as all conducts found in the parasphenoid of *Stanocephalosaurus amenasensis* seem to come from the arteria carotidis internae, they should belong to the arterial system. The following remaining identifications are also based on comparisons with *Rana* and *Salamandra* species (Gaupp, 1899; Francis, 1934) but they remain tentative because the pattern of the arteria carotidis internae is very variable, at least in anurans (Majorovà, 2003):

- The “anterior” conducts described above would correspond to the arteria palatina, supplying blood to the palatal area (Fig. 4). This hypothesis was also followed by Shishkin (1968) based on the arterial pattern observed in anurans (Gaupp, 1889). It is congruent with the direction of the conduct and its 3-D pattern reconstructed here, but differs from the “urodel model” in which no palatine arteria arise from the arteria carotis internae (Francis, 1934). Concerning

the most anterior conducts, they are smaller than the others and would correspond to bifurcating arterioles supplying the palatal area.

- As for the “dorsolateral” conducts opening toward the anterolateral borders of the parasphenoid (at the level of the conical recess margin, see Fig. 4), there is no satisfactory identification with respect to living amphibians (Gaupp, 1899; Francis, 1934). In *Lyrocephaliscus euri*, a dorsolateral conduct is described but not identified (Mazin & Janvier, 1983: fig. 7). Given the direction of these conducts reconstructed here, i.e. arising laterally from the parasphenoid, they could supply the prootic, situated just above. Or, if they turn anteriorly after arising from the parasphenoid as in *Lyrocephaliscus euri* (Mazin & Janvier, 1983: fig. 7), they could supply the palatal area through an opening between the epipterygoid and the pterygoid.

- “Ventrolateral” conducts are also reconstructed in *Stanocephalosaurus amenasensis*: they open ventrally toward the posterior part of the anterolateral margin of the parasphenoid (Fig. 4). Yet without identifying them, Shishkin (1973) mentioned similar small foramina in *Dvinosaurus egregius* which may be linked with these conducts and/or arterioles supplying the buccal mucous membrane.

The exoccipital of *Stanocephalosaurus amenasensis* also has several conducts and openings (Fig. 12): the lateral opening described above is also present in many species (e.g. *Benthosuchus sushkini*, *Lyrocephaliscus euri*, *Mastodonsaurus giganteus*), but its identification varies according to the authors: vagus nerve X in *Dvinosaurus primus* (Shishkin, 1973); glossopharyngeal nerve IX and nerve X in *Benthosuchus sushkini* (Bystrow & Efremov, 1940); nerve X and hypoglossal nerve XII in *Batrachosuchoides* (Shishkin & Sulej, 2009); or jugular vein in “*Stanocephalosaurus*” *pronus* (Howie, 1970). In *Stanocephalosaurus amenasensis*, the position and the large diameter of this lateral opening

suggests the jugular vein, as in its "*Stanocephalosaurus" pronus* relative. This interpretation is congruent with the internal jugular vein observed in anurans (Gaupp, 1899: fig. 119). The basal opening is also known in other temnospondyls such as *Siderops kehli* Warren & Hutchinson, 1983 where it is named the 'substapedial fossa' sensu Warren & Hutchinson (1983: 12) and in *Mastodonsaurus giganteus* where it is named the 'eustachian tube' sensu Schoch (2002: fig. 5). The name substapedial fossa is preferred here because the eustachian tube is restricted to mammals and its homology not proven. The lateral foramina are also frequent in temnospondyls: in *Stanocephalosaurus amenasensis*, two conducts, laterally located to the condyles, open above the processus submedullaris. This is also the case in *Edops craigi* (Romer & Witter, 1942), *Eryops megacephalus* (Sawin, 1941) and "*Stanocephalosaurus*" *pronus* (Howie, 1970) where these conducts are consensually assigned to branches 1 and 2 of the hypoglossal nerve XII. A third conduct is more problematic: located at the base of the processus paroticus in *Stanocephalosaurus amenasensis*, it leads to the posterior surface of the opisthotic. In *Paracyclotosaurus davidi*, a foramen assigned to hypoglossal nerve XII is located in a similar position, but no conduct has been described. In *Stanocephalosaurus amenasensis*, as this conduct links the opisthotic with the postcranial region, it would more likely be a vascular conduct.

The stapes of *Stanocephalosaurus amenasensis* also has a lateral foramen on the VPH (Fig. 9D, F). It is considered as a stapedial foramen by homology with those observed in many temnospondyls (e.g. *Edops craigi*, *Eryops megacephalus*, *Doleserpeton annectens*, *Benthosuchus sushkini)* and assigned to the stapedial artery. But the stapedial foramen of both *Edops craigi* and *Eryops megacephalus* is proportionally much larger than that of *Stanocephalosaurus amenasensis.*

At least, the epipterygoid of *Stanocephalosaurus amenasensis* has spaces between its processes, interpreted as areas of passage of nerves (Fig. 4): the ophtalmic branch V_1 of the trigeminal nerve between the processus basalis and processus dorsalis; and the maxillar branch V_2 and mandibular V_3 between the processus dorsalis and processus posterior (e.g. *Lyrocephaliscus euri*, Säve-Söderbergh, 1936), as hypothesised in many authors (e.g. Watson, 1958; Dutuit, 1976; Schoch, 2002).

Functional aspect of the stapes

Anatomy of the columellar cavity

Both stapes of *Stanocephalosaurus amenasensis* have their VPH fitting in the fenestra ovalis, but only the right one has an insertion process on the DPH which partly sutures the right crista parapterygoidea of the parasphenoid (Fig. 13A, B). The left DPH is close to the left crista parapterygoidea. The stapes is housed in a chamber delimited by the paroccipital process on the medial side, the crista obliqua, the lamina ascendens of the pterygoid, and the lamina descendens of the squamosal on the lateral side (Fig. 14). This chamber opens dorsally by the otic notch. The distal end of the stapes, by its position and its concave and rough surface, may be connected to a soft tissue layer in the otic notch. The posteromedial surface of the crista obliqua is rough, suggesting the insertion of a soft structure (Fig. 6E). This situation is very close to *Mastodontosaurus giganteus* (Schoch, 2000). As mentioned above, the crista obliqua forms a canal. The stapes is not housed in this canal but just above, and is not completely parallel to it: only the distal part of the shaft is parallel to the canal, the proximal part of the shaft crossing the crista obliqua. This situation looks similar in *Warrenisuchus aliciae* (Warren & Hutchinson, 1988) (Maganuco et al., 2009).

Mastodonsaurus giganteus also has an insertion process (Schoch, 2000) but only on the largest stapes, suggesting a development of this bone in a relatively late ontogenetic stage, at

least concerning its ossification. By contrast, in earlier ontogenetic stages, the VPH of *Mastodonsaurus* has a depression for a ball and socket joint, indicating mobility between the stapes and the parasphenoid (Schoch, 2000). Based on the fact that only one stapes of *Stanocephalosaurus amenasensis* is sutured (due to the presence of an insertion process), a similar situation is believed: the stapes is mobile during the pre-adult stages and then sutures the parasphenoid through ontogeny. This hypothesis is supported by the fact that temnospondyl long bones may continuously ossify through ontogeny, as revealed by skeletochronology (Steyer et al., 2004).

Role of the stapes

The role of the stapes is still debated: on one hand, it could function in support of the spiracle (Warren & Schroeder, 1995) which usually supplies water to the internal gills cavity and/or adjusts the water pressure between the gills, the columellar and buccal cavities to ensure a constant stream between them as in several species of living sharks (Hughes, 1960). In this case, as the stapes has a concave and rough distal end, the otic notch is presumed to be partially covered by soft tissue or by a spiracle valve, as in *Polypterus* (Graham et al. 2014). In *Stanocephalosaurus amenasensis*, this function does not appear to be realized for several reasons: 1) the insertion process of the stapes, when ossified (at a late ontogenetic stage), has only a partial suture zone which seems too weak for a support function; 2) this insertion process prevents a proximo-distal motion (Figs. 13-15), which is incompatible with a spiracle valve covering the otic notch; 3) the space between the distal end of the stapes and the skull roof is not sufficient to house muscles capable of moving a spiracle valve; and 4) there are no marks of muscular insertion on the stapes.

On the other hand, the role of the stapes could also be linked with the hearing system, as in most of the living anurans where this middle ear bone is situated in an air-filled cavity (e.g.

Bold & Lombard, 1985; Schoch, 2000). In this case, the stapes transmits sound waves from the tympanum covering the otic notch to the fenestra ovalis. A lever-system is also formed by an additional cartilaginous extra-stapes, which amplifies the acoustic vibrations. This hearing function, adapted to air-borne sounds, has been selected mostly in terrestrial taxa (e.g. *Rana temporaria* Linnaeus, 1758; see Jørgensen & Kanneworff, 1997; Wilczynski & Capranica, 1984). However, according to the dermo-sensory canals running along its skull roof, *Stanocephalosaurus amenasensis* was not terrestrial but aquatic (Dahoumane et al., 2016) or, at least, semiaquatic (Fortuny et al., 2011). And in temnospondyls, the stapes seems to be too massive to be moved by the vibration of a tympanum.

An aquatic hearing function of its stapes seems therefore possible, as in some living aquatic anurans (e.g. *Xenopus laevis* (Daudin, 1802), see Christensen-Dalsgaard & Elepfandt, 1995) In these taxa, the underwater hearing function of the stapes implies, in the middle ear, the presence of an air pocket acting as an amplification system for the acoustic vibrations (Hetherington & Lombard, 1982). This condition could be realized in *Stanocephalosaurus amenasensis* thanks to the columellar cavity whose anterior and lateral sides are formed by the concave and thin ascending flange of the pterygoid.

The insertion process is laterally situated on the stapes which prevents any proximo-distal displacement of the stapes. As described above, the fenestra ovalis is connected by the DPH laterally (and not by the VPH sub-vertically) which suggests that the stapes may transmit lateral vibrations (Figs. 13, 15). The VPH is aligned with the major axis of the columellar shaft but the DPH turns away from the major axis and fits into the fenestra ovalis. With a proximo-distal displacement, the force would be oriented toward the VPH which seems inefficient. With a lateral vibration transmitted from the air-pocket, the insertion process

could act as a hinge and the motion would orient the force toward the DPH, consequently toward the fenestra ovalis (Fig. 15).

The substapedial fossa of the stapes of *Stanocephalosaurus amenasensis* could also regulate the pressure in this putative air pocket by connecting the columellar cavity with the buccal cavity, thus fulfilling the role of the mammalian eustachian tube i.e. regulating air pressure in the pocket. In addition, the dorsoventrally flattened shape of the stapes suggests contact with the soft wall of this putative air chamber by providing a greater insertion surface. With this morphology, vibrations are directly transmitted from the soft wall to the stapes. At least, the soft tissue which may cover the otic notch (e. g. Schoch, 2000) could also provide a soft attachment structure of the distal extremity of the stapes in order to increase its mobility as sound receptor. Following this hypothesis, the entire skull would act as a global sound receptor transmitting the acoustic vibrations through its air-filled cavities, possibly with other slender bony elements like the flat lamina ascendens of the pterygoid.

Fusion of the stapes

The stapes completely sutures the parasphenoid in adults of *Lyrocephaliscus euri* (Säve-Söderbergh, 1936; Mazin & Janvier, 1983), *Eryops megacephalus* (Sawin, 1941), *Edops craigi* (Romer & Witter, 1942), *Dissorophus multicintus* (DeMar, 1968) and *Tersomius texensis* (Carroll, 1964), preventing any movements. If the ossification of the stapes is continuous through ontogeny (as demonstrated for long bones based on skeletochronology, see Steyer et al., 2004), this suggests a progressive reduction of the underwater hearing function of the stapes.

Evolution of the hearing system

This hypothesis of an underwater hearing stapes embedded in a soft air pocket questions the polarization and tempo acquisition of the associated characters: as a spiracle has already been

highlighted in *Acanthostega gunnari* Jarvik, 1952 (Clack, 1989), and an air-filled resonance cavity hypothesized in *Ichthyostega* which owns a spoon-like stapes (Clack, 2003), the putative soft air pocket of *Stanocephalosaurus* (and possibly other temnospondyls, see below) could derive from the early tetrapod spiracle. However, the double-headed morphology of the stapes as well as its insertion process and the dorso-ventrally flattening are also visible in various temnospondyls such as the basal *Edops craigi* (Romer & Witter, 1942) and the advanced *Lyrocephaliscus euri* (Mazin & Janvier, 1983) or *Mastodonsaurus giganteus* (Schoch, 1999a). This possible hearing function of the stapes may therefore appear during the early evolution of temnospondyls, yet with some exceptions (or reversion): in *Eryops craigi*, the distal end of the stapes points toward the tabular rather than the otic notch (Sawin, 1941), and in *Iberospondylus schultzei* Laurin & Soler-Gijón, 2001, the otic notch is occluded by an otic flange (Laurin & Soler-Gijón, 2006). Whatever the function is, these different morphologies could be coded in several character states in order to be used in phylogenetic analyses, but more comparisons between different taxa are needed.

At least, considering the close relationships between temnospondyls and lissamphibians (e.g. Milner, 1993; Ruta et al., 2007; and various authors), this possible early appearance of the tympanic membrane (possibly from a soft tissue covering the otic notch), the tympanic annulus (possibly from the dorsal process of the quadrate; see Bolt & Lombard, 1985), and the extrastapes could be related to the common anuran hearing system.

Conclusion

This exceptionally well-preserved specimen of *Stanocephalosaurus amenasensis* gives access to an unparalleled degree of anatomical detail, completing our knowledge of the temnospondyl endocranium. Endocranial exploration using X-ray micro-CT scan, leads to the observation of structures like the otic capsule, rarely preserved and/or hardly accessible by

classical manual preparation. Moreover, unique morphological features have been observed, such as the delta-groove of the exoccipital, and parts of the arterial and nervous systems have been newly reconstructed.

Such detailed morphology and conservation of the shape are also of paleobiological interest: it allows the function of the stapes to be reinterpreted as part of a possible underwater hearing system including an air pocket acting as resonance chamber. A comparison with early tetrapods and other temnospondyls suggests this possible function could appear early in tetrapod evolution. Of course further analyses are needed to confirm or not this hypothesis, but this study shows that endocranial investigations of well-preserved specimens provide fascinating perspectives on our understanding of temnospondyl paleobiology and evolution.

Acknowledgements

We thank P. Ahlberg (Uppsala University, Sweden) and R. R. Schoch (Staatliches Museum für Naturkunde, Stuttgart, Germany) for their useful discussions; F. Goussard (CR2P, Paris, France) for his help and advices on 3-D reconstructions; P. Janvier (CR2P - Académie des Sciences, Paris) for its proof readings and advices; G. Clément (CR2P) for its proof readings; D. Germain (CR2P) for access to comparative specimens of the MNHN collections; L. Cazes (CR2P) for the photos; Renaud Vacant (CR2P) for the preparation and the cast of the specimen ZAR05; the Editor Louise Allcock and two anonymous referees for their useful reviews.

References

Aït Ouali R, Nedjari A, Taquet P, Bitam L, Tayeb Cherif L, Bouras R. 2011. Le Zarzaïtine Inférieur : derniers développements dans une série du Trias pro-parte. *Mémoires du Service Géologique National* 17: 6-26.

Amalitskii VP. 1921. Severodvinian Excavations of prof. VP. Amalitskii: 1. *Akademii Nauk Press, Petrograd* 1-16.

Balanoff A. 2011. Oviraptorosauria: Morphology, phylogeny, and endocranial evolution. D. Phil. Thesis, Columbia University.

Bolt JR. 1969. Lissamphibian origins: possible protolissamphibian from the Lower Permian of Oklahoma. *Science* 166: 888-891.

Bolt JR, Lombard RE. 1985. Evolution of the amphibian tympanic ear and the origin of frogs. *Biological Journal of the Linnean Society* 24: 83-99.

Bystrow AP, Efremov JA. 1940. *Benthosuchus sushkini* - a labyrinthodont from the Eotriassic of Sharzhenga River. *Trudy Paleozoologicheskogo Instituta Akademii Nauk SSSR* 10: 1-152.

Carroll RL. 1964. Early evolution of the dissorophid amphibians. *Bulletin of the Museum of Natural History Harvard University* 131: 161-250.

Carroll RL. 2007. The Palaeozoic ancestry of salamanders, frogs and caecilians. *Zoological Journal of the Linnean Society* 150: 1-140.

Case EC. 1910. New or little known reptiles and amphibians from the Permian of New Mexico. *Bulletin of the American Museum of Natural History* 38: 163-196.

Christensen-Dalsgaard J, Elepfandt A. 1995. Biophysics of underwater hearing in the clawed frog, *Xenopus laevis*. *Journal of Comparative Physiology A* 176: 317-324.

Clack JA. 1989. Discovery of the earliest-known tetrapod stapes. *Nature* 342: 425-427.

Clack JA, Ahlberg PE, Finney SM, Alonso PD, Robinson J, Ketcham RA. 2003. A uniquely specialized ear in a very early tetrapod. *Nature* 425: 65-69.

Cope ED. 1877. Descriptions of extinct Vertebrata from the Permian and Triassic Formations of the United States. *Proceedings of the American Philosophical Society* 17: 182-193.

Cope ED. 1878. Description of extinct Batrachia and Reptilia from the Permian Formation of Texas. *Proceedings of the American Philosophical Society* 17: 505-530.

Cope ED. 1895. A batrachian armadillo. *American Naturalist* 29: 998.

Dahoumane A, Nedjari A, Aït Ouali R, Taquet P, Vacant R, Steyer J-S. 2016. A new mastodonsauroid temnospondyl from the Triassic of Algeria: implications for the

biostratigraphy and palaeoenvironments of the Zarzaïtine Series, Northern Sahara. *Comptes Rendus Palevol* 15: 918-926; doi:10.1016/j.crpv.2015.09.005.

Damiani RJ. 2001. A systematic revision and phylogenetic analysis of Triassic mastodonsauroids (Temnospondyli: Stereospondyli). *Zoological Journal of the Linnean Society* 133: 379-482.

DeMar R. 1968. The Permian labyrinthodont amphibian *Dissorophus multicinctus*, and adaptations and phylogeny of the family Dissorophidae. *Journal of Paleontology* 42: 1210-1242.

Dutuit JM. 1976. Introduction à l'étude paléontologique du Trias continental marocain. Description des premiers Stégocephales recueillis dans le Couloir d'Argana (Atlas Occidental). *Mémoires du Muséum National d'Histoire Naturelle, Série C, Sciences de la Terre* 36: 1-253.

Efremov IA. 1929. *Benthosaurus sushkini*, ein neuer Labyrinthodont der permotriassischen Ablagerungen der Sharschenga Flusses. *Trudy Paleozoologicheskogo Instituta Akademii Nauk SSSR* 1929: 757-770.

Fraas E. 1913. Neue Labyrinthodonten aus der schwäbischen Trias. *Palaeontographica* 60: 275-294.

Francis ETB. 1934. *The anatomy of the salamander*. Ithaca, New York: Society for the Study of Amphibians and Reptiles.

Fortuny F, Marcé-Nogué J, de Esteban-Trivigno S, Galobart À. 2011. Temnospondyli bite club: ecomorphological patterns of the most diverse group of early tetrapods. *Journal of Evolutionary Biology* 24: 2040-2054.

Gaupp E. 1899. *A. Ecker and R. Wiedersheim's Anatomie des frosches, Vol. 2*. Braunschweig: Friedrich Vieweg und Sohn.

Graham JB, Wegner NC, Miller LA, Jew CJ, Lai NC, Berquist RM, Frank L, Long JA. 2014. Spiracular air breathing in polypterid fishes and its implications for aerial respiration in stem tetrapods. *Nature communications* 5: 1-6; doi:10.1038/ncomms4022.

Hetherington TE, Lombard RE. 1982. Biophysics of underwater hearing in anuran amphibians. *Journal of Experimental Biology* 98: 49-66.

Howie AA. 1970. A new capitosaurid labyrinthodont from East Africa. *Palaeontology* 13: 210-253.

Hughes GM. 1960. The mechanism of gill ventilation in the dogfish and skate. *Journal of Experimental Biology* 37: 11-27.

Jaeger GF. 1828. Über die fossile Reptilien, welche in Württemberg aufgefunden worden sind. Stuttgart: J. B. Metzler.

Jarvik E. 1952. On the fish-like tail in the ichthyostegid stegocephalians with descriptions of a new stegocephalian and a new crossopterygian from the Upper Devonian of East Greenland. *Meddelelser om Grønland* 114: 1-90.

Jørgensen MB, Kanneworff M. 1997. Middle ear transmission in the grass frog, *Rana temporaria*. *Journal of Comparative Physiology A* 182: 59-64.

Laurin M, Reisz R. 1997. A new perspective on tetrapod phylogeny. In: Sumida SS, Martin KL, eds. *Amniote origins*. New York: Academic Press, 9-59.

Laurin M, Soler-Gijón R. 2001. The oldest stegocephalian from the Iberian Peninsula: evidence that temnospondyls were euryhaline. *Comptes Rendus de l'Académie des Sciences, Series III, Sciences de la Vie* 324: 495-501.

Laurin M, Soler-Gijón R. 2006. The oldest known stegocephalian (Sarcopterygii: Temnospondyli) from Spain. *Journal of Vertebrate Paleontology* 26: 284-299.

Linnaeus C. 1758. Systema naturae, 10th eds, vol. 1. Stockholm: Laurentii Salvii.

Lombard RE, Bolt JR. 1988. Evolution of the stapes in Paleozoic tetrapods. In: Fritzsch B, Ryan MJ, Wilczynski W. Hetherington TE, Walkowiak W, eds. *Evolution of the amphibian auditory system*. New York: Wiley & Sons, 37-67.

Macrini TE, Rowe T, Archer M. 2006. Description of a cranial endocast from a fossil platypus, Obdurodon dicksoni (Monotremata, Ornithorhynchidae), and the relevance of endocranial characters to monotreme monophyly. *Journal of Morphology* 267: 1000-1015.

Maganuco S, Steyer, JS, Pasini G, Boulay M, Lorrain S, Bénéteau A, Auditore M. 2009. An exquisite specimen of *Edingerella madagascarensis* (Temnospondyli) from the Lower Triassic of NW Madagascar; cranial anatomy, phylogeny, and restorations. *Memorie della Società Italiana di Scienze Naturali e del Museo Civico di Storia Naturale di Milano* 36: 1-72.

Majorovà H. 2003. Transformation of the arterial arches in the course of amphibian metamorphosis. Unpublished Master thesis, Charles University, Prague.

Mazin JM, Janvier P. 1983. L'anatomie de *Lyrocephaliscus euri* (Wiman), trématosaure du Trias Inférieur du Spitsberg: arrière-crane, squelette axial et ceinture scapulaire. *Palaeovertebrata* 13: 13-31.

Meyer E. 1842. Labyrinthodonten-Genera. *Neues Jahrbuch für Mineralogie, Geographie, Geologie, Paläontologie* 1842: 301-304.

Milner AR.1993. The Paleozoic relatives of lissamphibians. *Herpetological Monographs* 7: 8-27.

Nedjari A, Aït Ouali R, Bitam L, Steyer J-S, Taquet P, Vacant R, Bouzidi W, Kedadra, B. 2010. Découverte d'un nouveau gisement de stégocéphales d'une conservation exceptionnelle dans le Trias d'in Amenas (bassin d'Illizi, Algérie). *Bulletin du Service Géologique National* 21: 1-18.

Owen R. 1853. Notes on the above-described fossil remains. *Quarterly Journal of the Geological Society of London* 9: 66-67.

Piveteau J. 1955. *Traité de Paléontologie, Tome V: Amphibiens, Reptiles, Oiseaux*. Paris: Masson.

Robinson J, Ahlberg PE, Koentges G. 2005. The braincase and middle ear region of *Dendrerpeton acadianum* (Tetrapoda: Temnospondyli). *Zoological Journal of the Linnean Society* 143: 577-597.

Romer AS. 1936. Studies on American Permo-Carboniferous reptiles. *Problems of Paleontology* 1: 85-93.

Romer AS, Witter RV. 1942. *Edops*, a primitive rachitomous amphibian from the Texas Red Beds. *Journal of Geology* 50: 925-959.

Ruta M, Coates MI. 2007. Dates, nodes and character conflict: addressing the lissamphibian origin problem. *Journal of Systematic Palaeontology* 5: 69-122.

Säve-Söderbergh G. 1936. On the morphology of Triassic stegocephalians from Spitsbergen, and the interpretation of the endocranium in the Labyrinthodontia. *Kunglik Svensk Vetenskapsakademiens Handlingar* 16: 1-181.

Sawin HJ. 1941. The cranial anatomy of *Eryops megacephalus*. *Bulletin of the Museum of Comparative Zoology* 88: 407-463.

Schoch RR. 1999a. Comparative osteology of *Mastodonsaurus giganteus* (Jaeger, 1828) from the Middle Triassic (Letten- keuper: Longobardian) of Germany (Baden-Württemberg, Bayern, Thüringen). *Stuttgarter Beiträge zur Naturkunde B* 278: 1-175.

Schoch RR. 1999b. Studies on braincases of early tetrapods: structure, morphological diversity, and phylogeny - 1. *Trimerorachis* and other primitive temnospondyls. *Neues Jahrbuch für Geologie und Paläontologie, Abhandlungen* 213: 233-259.

Schoch RR. 2000. The stapes of *Mastodonsaurus giganteus* (Jaeger 1828) - structure, articulation, ontogeny, and functional implications. *Neues Jahrbuch für Geologie und Paläontologie, Abhandlungen* 215: 177-200.

Schoch RR. 2002. The neurocranium of the stereospondyl *Mastodonsaurus giganteus*. *Palaeontology* 45: 627-645.

Schoch RR, Milner AR. 2000. Stereospondyli. In: Wellnhofer P, eds. *Handbuch der Paläoherpetologie*, Vol. 3B. Munich: Pfeil, 1-203.

Shishkin MA. 1968. On the cranial arterial system of the labyrinthodonts. *Acta Zoologica* 49: 1-22.

Shishkin MA. 1973. The morphology of the early Amphibia and some problems of lower tetrapod evolution. *Trudy Paleozoologicheskogo Instituta* 137: 1-257.

Shishkin MA, Sulej T. 2009. Early Triassic temnospondyls of the Czatkowice 1 tetrapod assemblage. *Palaeontologia Polonica* 65: 31-77.

Sigurdsen T. 2008. The otic region of *Doleserpeton* (Temnospondyli) and its implications for the evolutionary origin of frogs. *Zoological Journal of the Linnean Society* 154: 738-751.

Steyer JS. 2000. Ontogeny and phylogeny in temnospondyls: a new method of analysis. *Zoological journal of the Linnean Society* 130: 449-467.

Steyer JS, Laurin M, Castanet J, de Ricqlès A. 2004. First histological and skeletochronological data on temnospondyl growth: palaeoecological and palaeoclimatological implications. *Palaeogeography, Palaeoclimatology, Palaeoecology* 206: 193-201.

Steyer JS, Damiani R. 2005. A giant brachyopoid temnospondyl from the Upper Triassic or Lower Jurassic of Lesotho. *Bulletin de la Société Géologique de France* 176: 243-248.

Sulej T. 2007. Osteology, variability, and evolution of *Metoposaurus*, a temnospondyl from the Late Triassic of Poland. *Palaeontologia Polonica* 64: 29-139.

Warren A. 2000. Secondarily aquatic temnospondyls of the Upper Permian and Mesozoic. *In:* Heatwole H, Carroll R, eds. *Amphibian biology*, Vol. 4, *Palaeontology: the evolutionary history of amphibians.* Chipping Norton, Australia: Surrey Beatty & Sons, 1121-1149.

Warren AA, Hutchinson MN. 1983. The last labyrinthodont? A new brachyopoid (Amphibia, Temnospondyli) from the early Jurassic Evergreen Formation of Queensland, Australia. *Philosophical Transactions of the Royal Society of London B: Biological Sciences* 303: 1-62.

Warren AA, Hutchinson MN. 1988. A new capitosaurid amphibian from the Early Triassic of Queensland, and the ontogeny of the capitosaur skull. *Palaeontology* 31: 857-876.

Warren AA, Schroeder N. 1995. Changes in the capitosaur skull with growth: an extension of the growth series of *Parotosuchus aliciae* (Amphibia, Temnospondyli) with comments on the otic area of capitosaurs. *Alcheringa* 19: 41-46.

Watson DMS. 1958. A new labyrinthodont (*Paracyclotosaurus*) from the Upper Trias of New South Wales. *Bulletin of the British Museum (Natural History) Geology* 3: 233-263.

Watson DMS. 1962. The evolution of the labyrinthodonts. *Philosophical Transactions of the Royal Society of London B: Biological Sciences* 245: 219-265.

Wilczynski, W, Capranica RR.1984. The auditory system of anuran amphibians. *Progress in neurobiology* 22: 1-38.

Wiman C. 1914. Über die Stegocephalen aus der Trias Spitzbergens. *Bulletin of the Geological Institute of the University of Uppsala* 13: 1-34.

Witzmann F, Schoch RR, Hilger A, Kardjilov N. 2012. Braincase, palatoquadrate and ear region of the plagiosaurid *Gerrothorax pulcherrimus* from the Middle Triassic of Germany. *Palaeontology* 55: 31-50.

Yates AM, Warren AA. 2000. The phylogeny of the 'higher' temnospondyls (Vertebrata: Choanata) and its implications for the monophyly and origins of the Stereospondyli. *Zoological Journal of the Linnean Society* 128: 77-121.

Figure Captions

Figure 1. Dorsal view of *Stanocephalosaurus amenasensis* (specimen ZAR05) from the Lower/Middle Triassic of Algeria. Scale bar = 30 mm.

Figure 2. 3-D model of *Stanocephalosaurus amenasensis* (specimen ZAR05) produced with Mimics® 17.0. A, dorsal view. B, dorsal view with skull roof removed. Scale bar = 30 mm.

Figure 3. Parasphenoid of *Stanocephalosaurus amenasensis* (specimen ZAR05) produced with Mimics® 17.0. A, dorsal view. B, ventral view. C, right lateral view. D, left lateral view. E, anterior view. F, posterior view. Scale bar = 20 mm.

Figure 4. Posterodorsal view of the parasphenoid of *Stanocephalosaurus amenasensis* (specimen ZAR05) produced with Mimics® 17.0 with internal conducts seen by transparency. Scale bar = 20 mm.

Figure 5. Epipterygoid of *Stanocephalosaurus amenasensis* (specimen ZAR05) produced with Mimics® 17.0. A, anterior view. B, posterior view. C, medial view. D, lateral view. E, dorsal view. F, ventral view. Scale bar = 20 mm.

Figure 6. Pterygoid of *Stanocephalosaurus amenasensis* (specimen ZAR05) produced with Mimics® 17.0. A, dorsal view. B, ventral view. C, anterior view. D, posterior view. E, medial view. F, lateral view. Scale bar = 20 mm.

Figure 7. Right prootic of *Stanocephalosaurus amenasensis* (specimen ZAR05) produced with Mimics® 17.0. A, anterior view. B, posterior view. C, lateral view. D, dorsal view. E, ventral view. F, medial view. Scale bar = 10 mm.

Figure 8. Left opisthotic of *Stanocephalosaurus amenasensis* (specimen ZAR05) produced with Mimics® 17.0. A, anterior view. B, posterior view. C, ventral view. D, lateral view. E, medial view. F, dorsal view. Scale bar = 10 mm.

Figure 9. Right stapes of *Stanocephalosaurus amenasensis* (specimen ZAR05) produced with Mimics® 17.0. A, lateral view. B, medial view. C, anterior view. D, posterior view. E, dorsal view. F, ventral view. Scale bar = 20 mm.

Figure 10. Exoccipital of *Stanocephalosaurus amenasensis* (specimen ZAR05) produced with Mimics® 17.0. A, posterior view. B, anterior view. C, dorsal view. D, ventral view. E, right lateral view. F, left lateral view. Scale bar = 20 mm.

Figure 11. Anterior view of the occipital area showing the delta groove of *Stanocephalosaurus amenasensis* (specimen ZAR05) produced with Mimics® 17.0. For legends, see Figure 1. Scale bar = 20 mm.

Figure 12. Posterolateral view of the exoccipital of *Stanocephalosaurus amenasensis* (specimen ZAR05) produced with Mimics® 17.0 with internal conduct seen by transparency. Scale bar = 20 mm.

Figure 13. Posterior part of the 3-D model of *Stanocephalosaurus amenasensis* (specimen ZAR05) produced with Mimics® 17.0. A, lateral view, with stapes removed. B, lateral view with stapes in place. Red double-arrow corresponds to the possible proximo-distal displacement motion, yellow double-arrow corresponds to the possible lateral vibration motion. For legends, see Figure 1. Scale bar = 15 mm.

Figure 14. Dorsal view of the 3-D model of *Stanocephalosaurus amenasensis* (specimen ZAR05) produced with Mimics® 17.0, skull roof removed. For legends, see Figure 1. Scale bar = 30 mm.

Figure 15. Dorsal view of the right columellar cavity of *Stanocephalosaurus amenasensis* (specimen ZAR05) produced with Mimics® 17.0 showing possible motions (double-arrows) and applied forces (simple-arrows). Red double-arrow corresponds to the proximo-distal displacement motion, yellow double-arrow corresponds to lateral vibration motion, simple arrows correspond to the respective applied forces. For legends, see Figure 1. Scale bar = 20 mm.

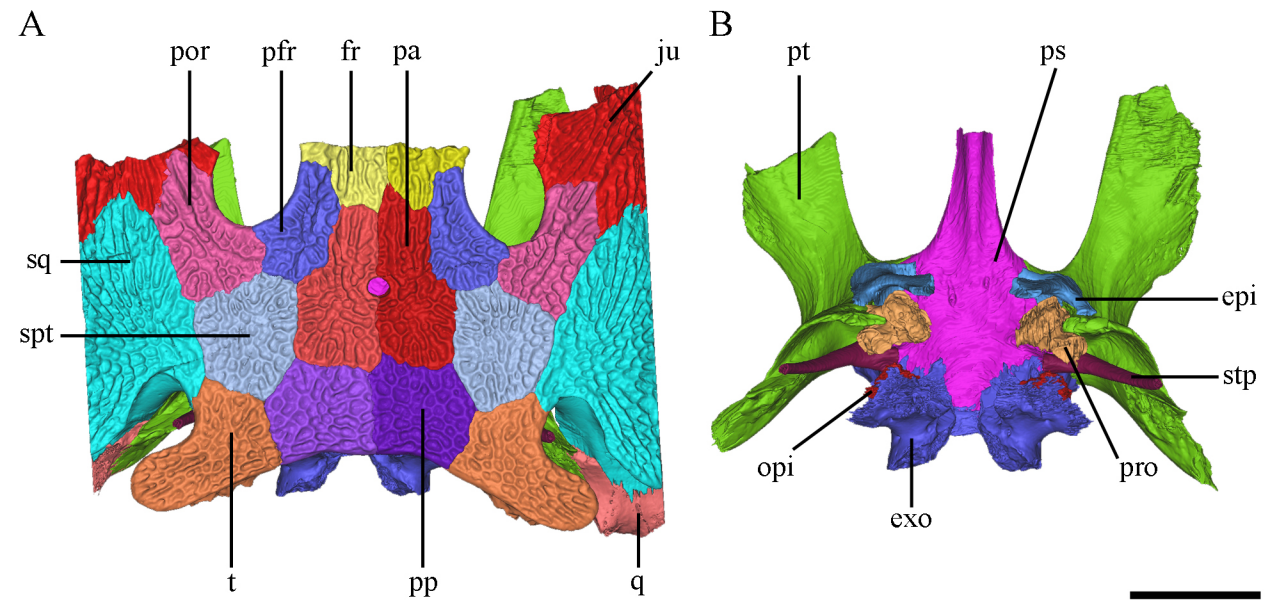
A
por
pfr
fr
pa
ju
sq
spt
t
pp
q
B
pt
ps
epi
stp
opi
pro
exo

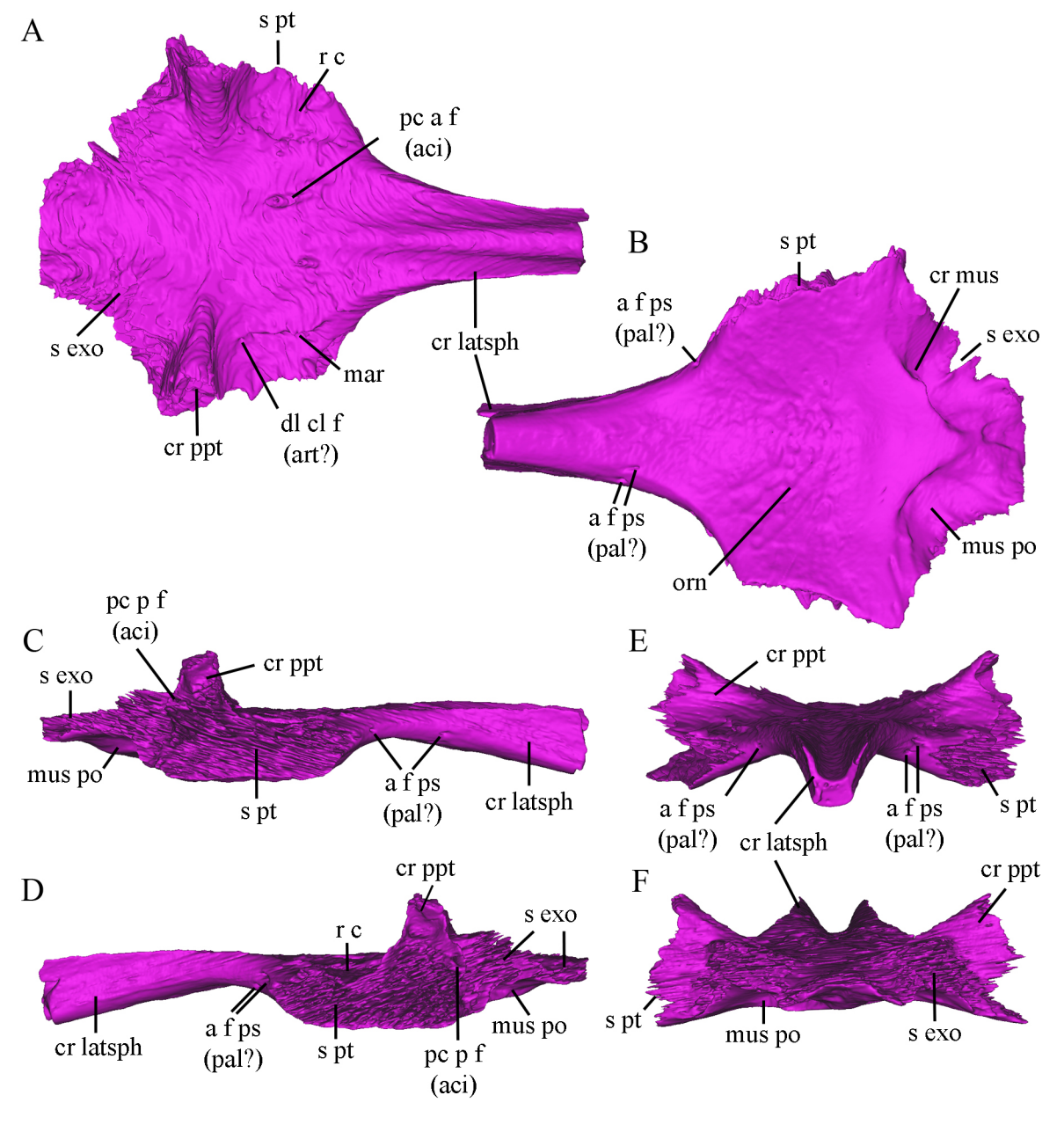
A
s pt
r c
pc a f
(aci)
s exo
mar
cr latsph
dl cl f
(art?)
cr ppt
B
s pt
cr mus
a f ps
(pal?)
s exo
a f ps
(pal?)
mus po
orn
C
pc p f
(aci)
cr ppt
s exo
mus po
s pt
a f ps
(pal?)
cr latsph
E
cr ppt
a f ps
(pal?)
cr latsph
a f ps
(pal?)
s pt
D
cr ppt
r c
s exo
cr latsph
a f ps
(pal?)
s pt
mus po
pc p f
(aci)
F
cr ppt
s pt
mus po
s exo

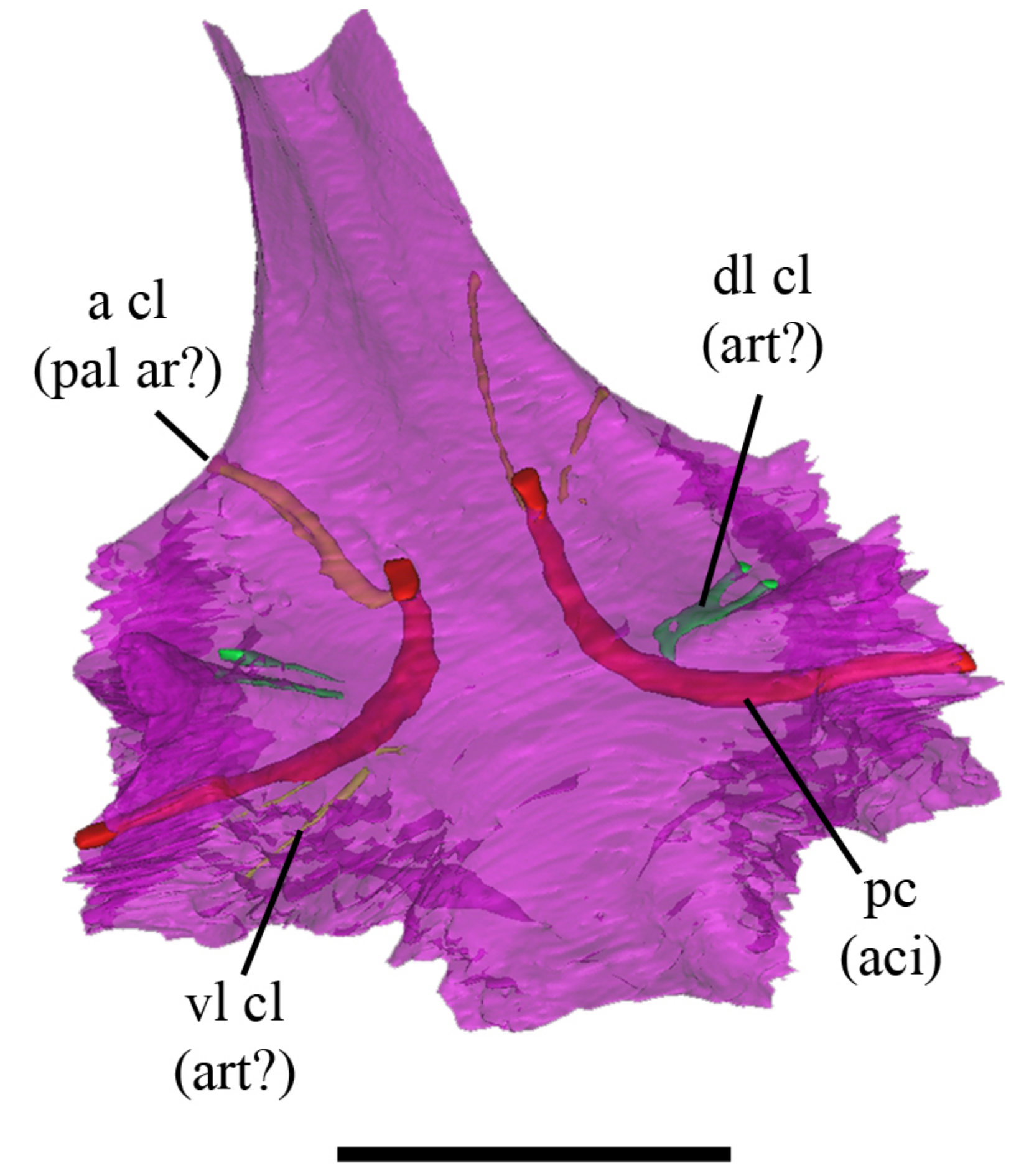
a cl
(pal ar?)
dl cl
(art?)
pc
(aci)
vl cl
(art?)

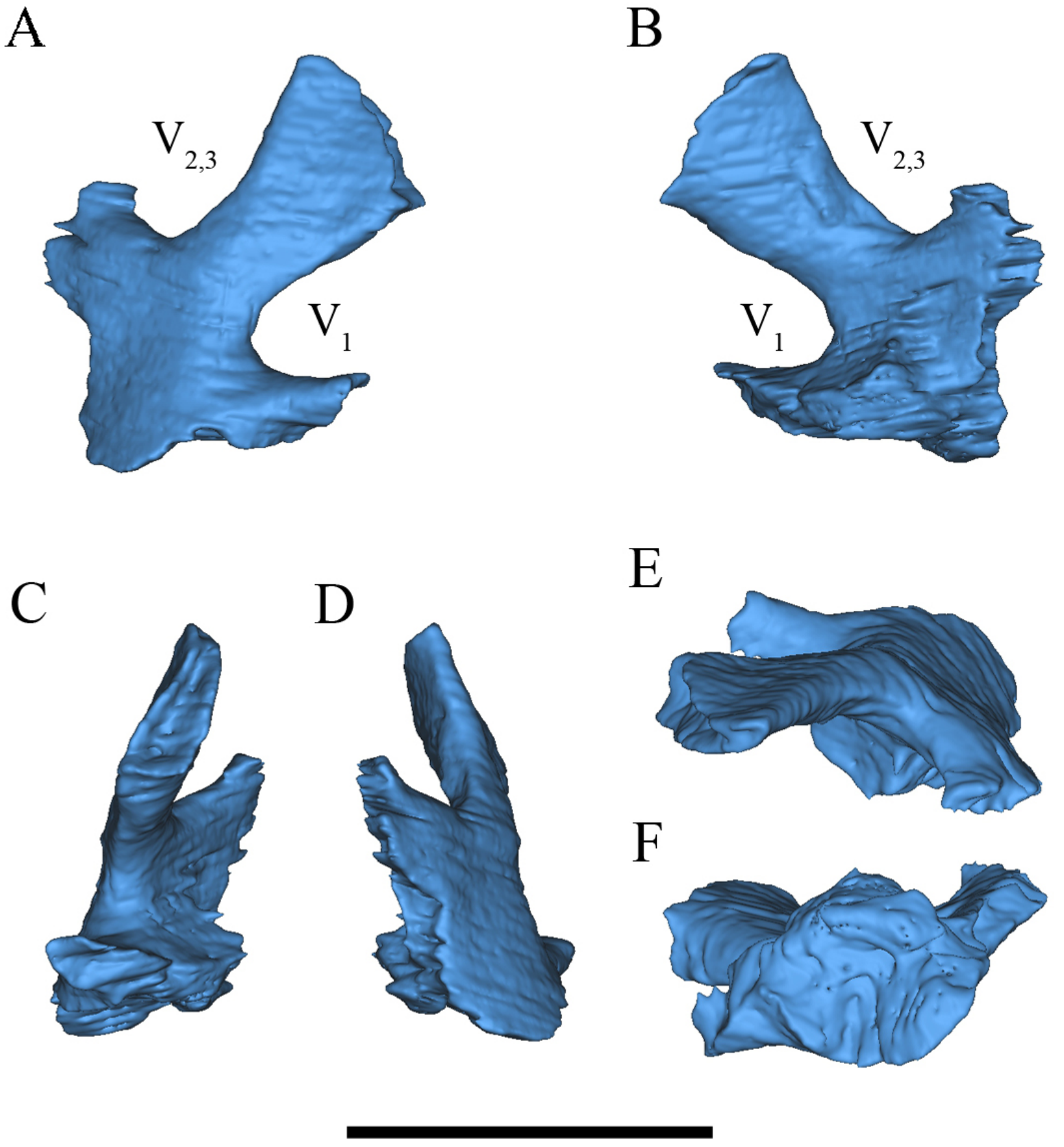
A
V2,3
V1
B
V2,3
V1
C
D
E
F

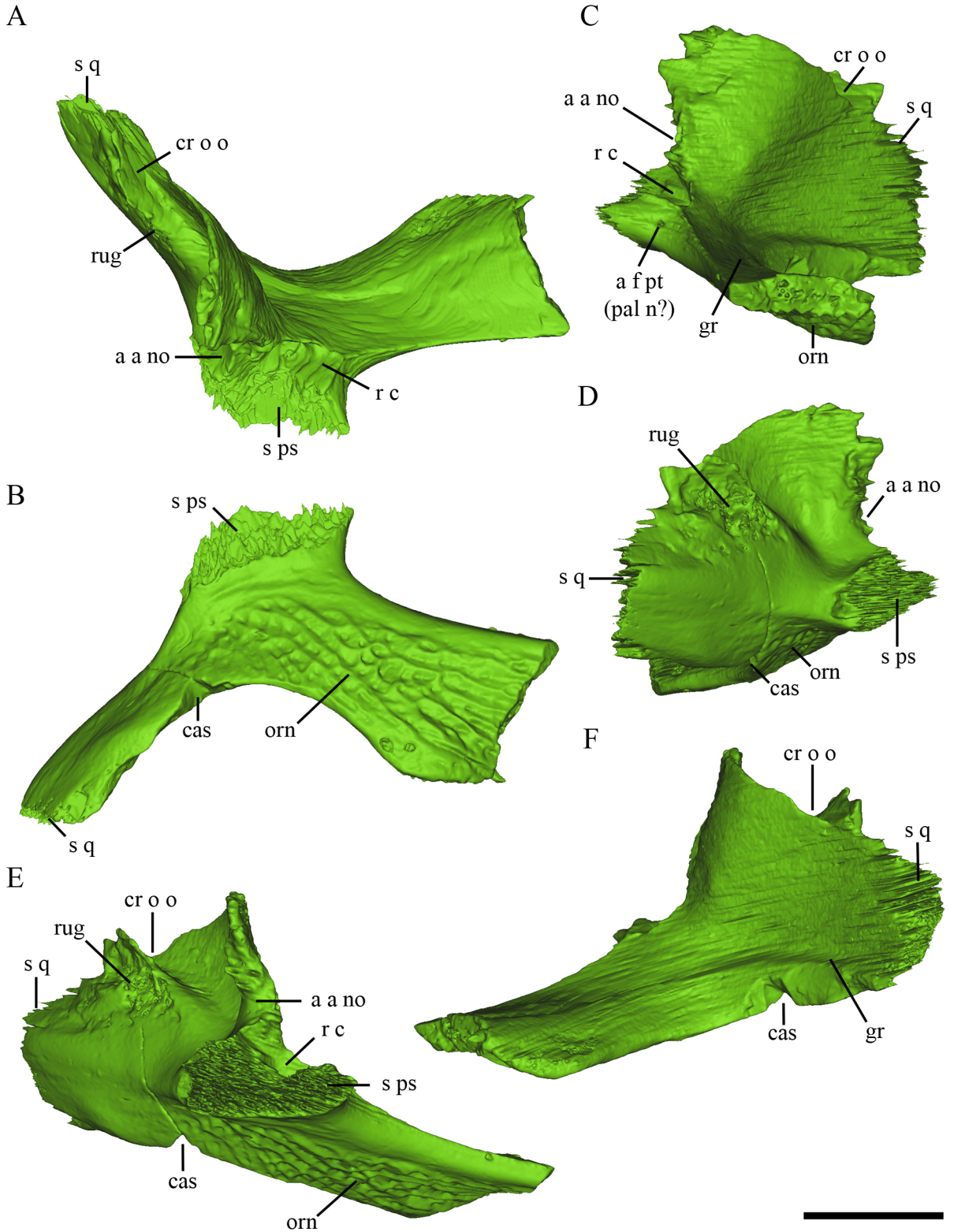
A
s q
cr o o
rug
a a no
r c
s ps
B
s ps
cas
orn
s q
C
cr o o
a a no
s q
r c
a f pt
(pal n?)
gr
orn
D
rug
a a no
s q
s ps
orn
cas
E
cr o o
rug
s q
a a no
r c
s ps
cas
orn
F
cr o o
s q
cas
gr

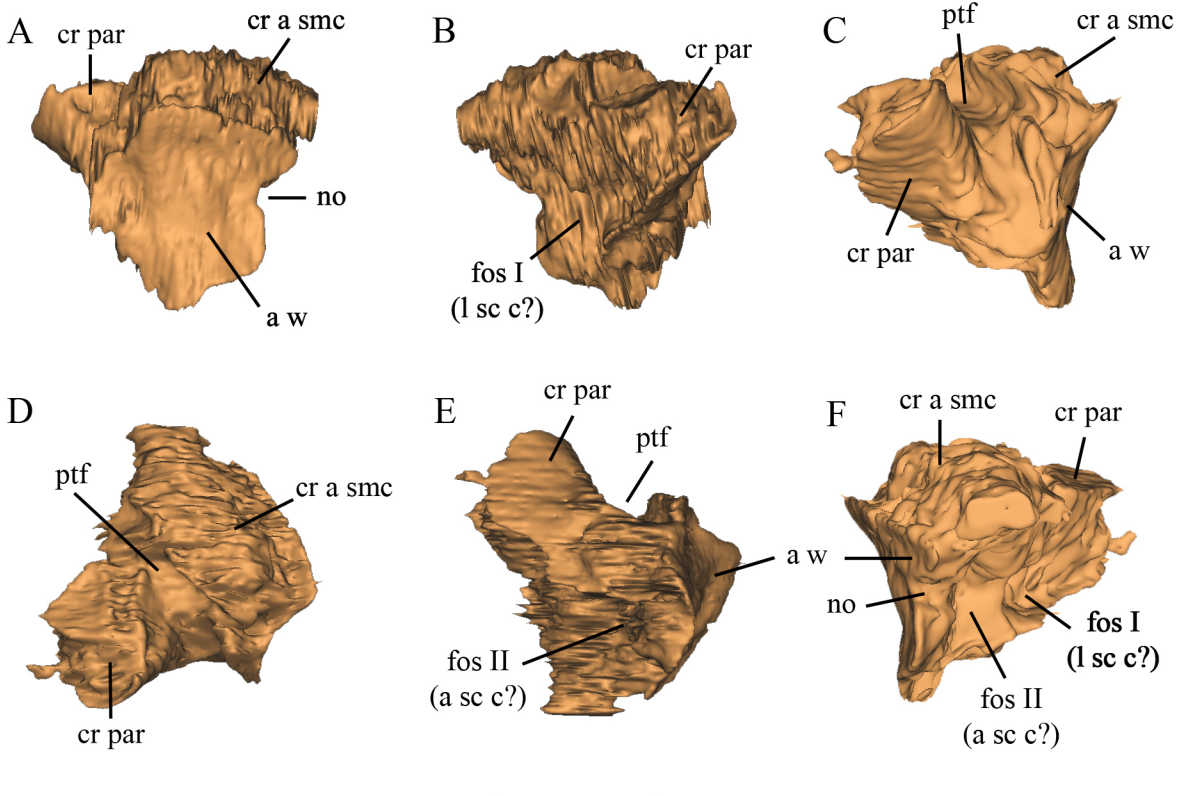
A
cr par
cr a smc
no
a w
B
cr par
fos I
(l sc c?)
C
ptf
cr a smc
cr par
a w
D
ptf
cr a smc
cr par
E
cr par
ptf
a w
fos II
(a sc c?)
F
cr a smc
cr par
a w
no
fos I
(l sc c?)
fos II
(a sc c?)

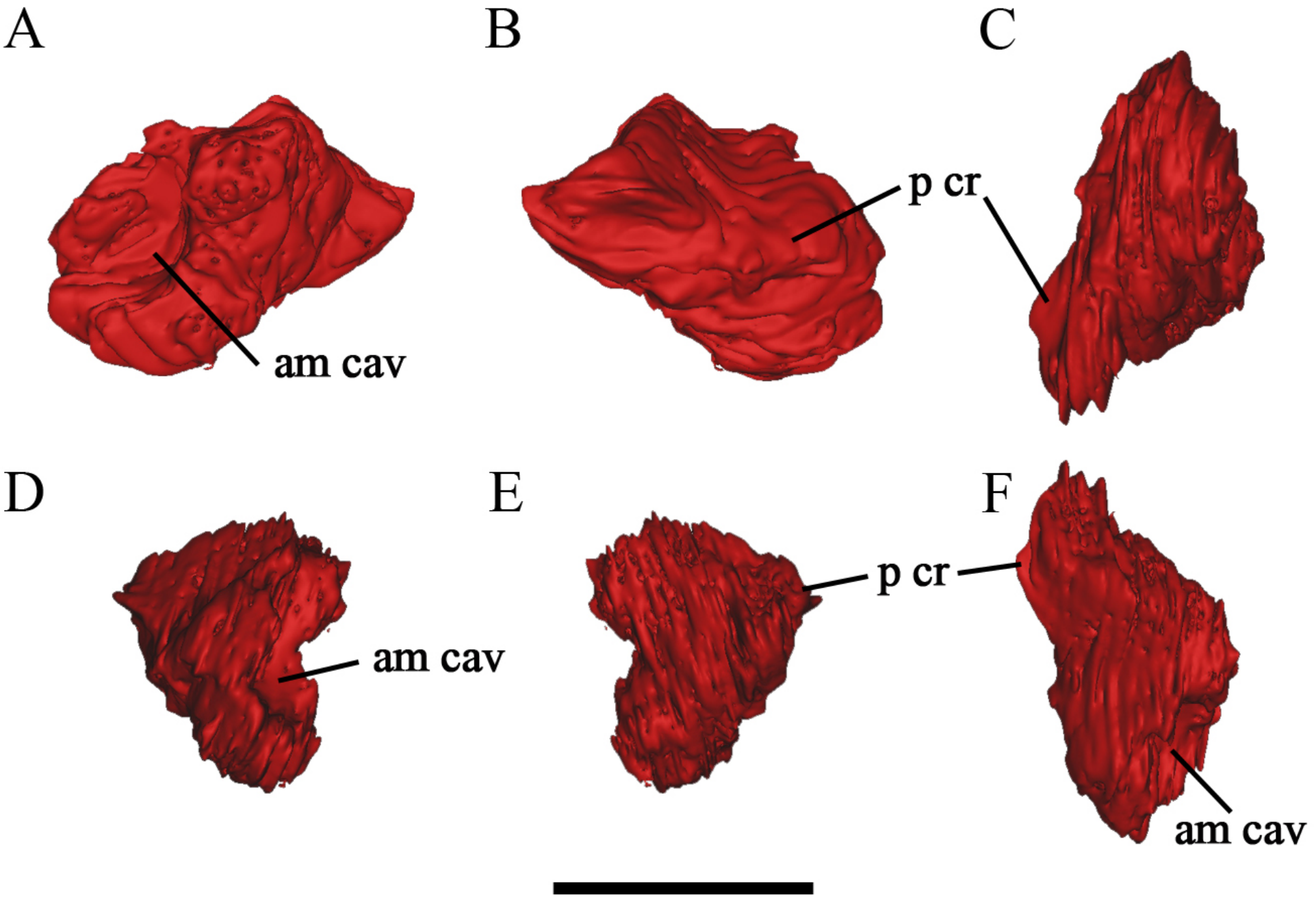
A
am cav
B
p cr
C
D
am cav
E
p cr
F
am cav

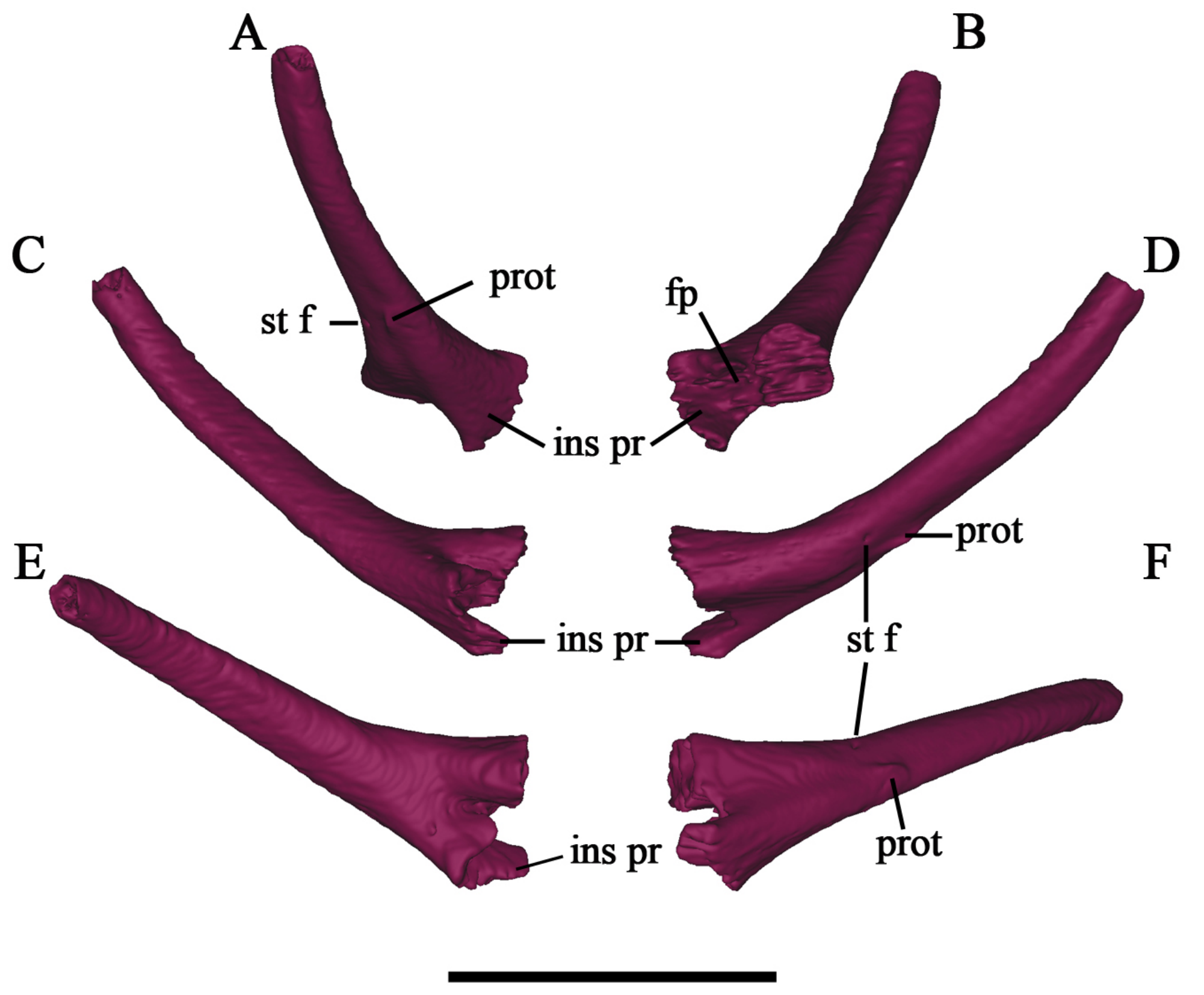
A
B
C
D
E
F
prot
st f
fp
ins pr
ins pr
prot
st f
ins pr
prot

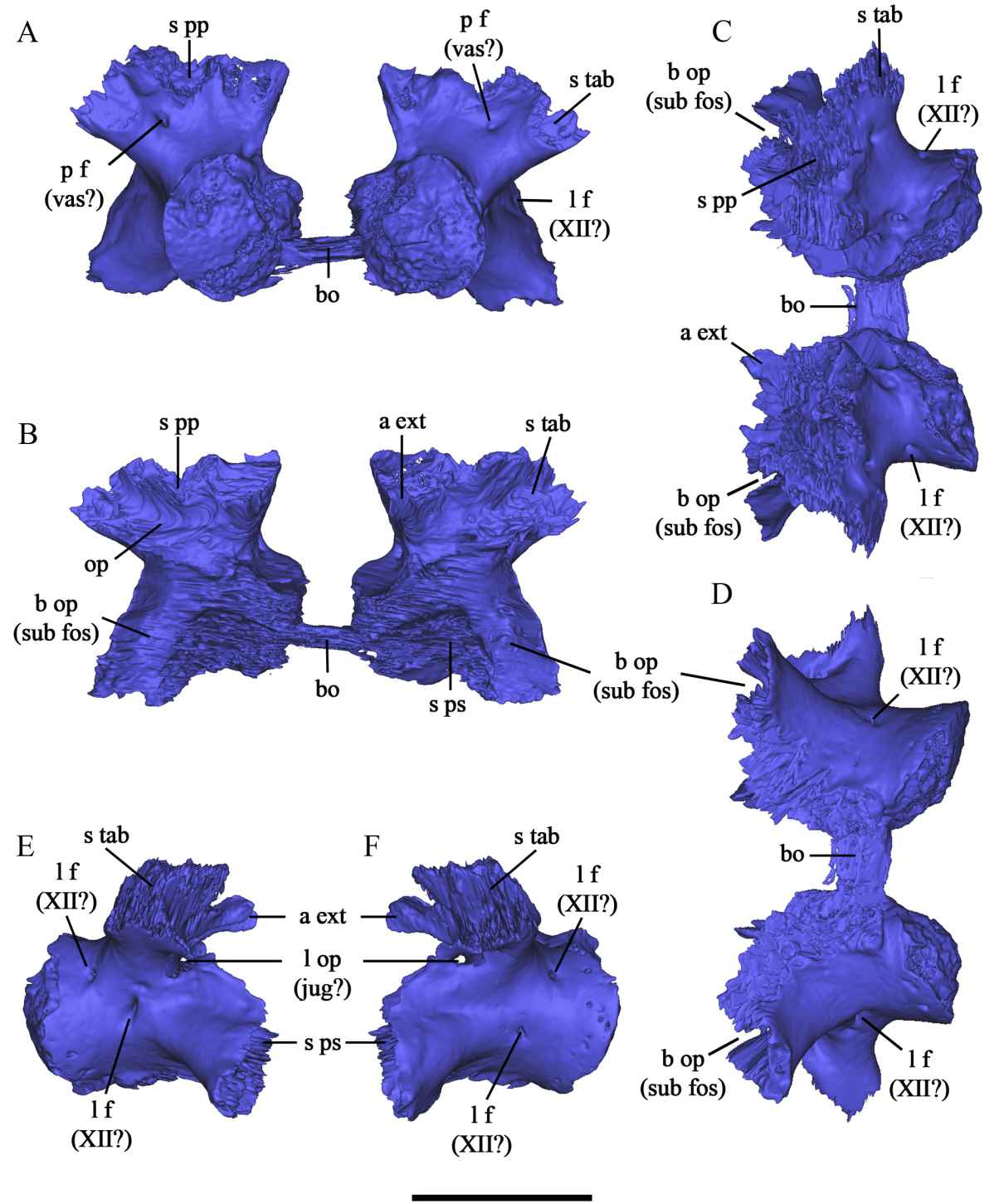
A
s pp
p f
(vas?)
s tab
p f
(vas?)
l f
(XII?)
bo
B
s pp
a ext
s tab
op
b op
(sub fos)
bo
s ps
C
s tab
b op
(sub fos)
l f
(XII?)
s pp
bo
a ext
b op
(sub fos)
l f
(XII?)
D
l f
(XII?)
b op
(sub fos)
bo
b op
(sub fos)
l f
(XII?)
E
s tab
l f
(XII?)
a ext
l op
(jug?)
s ps
l f
(XII?)
F
s tab
l f
(XII?)
l f
(XII?)

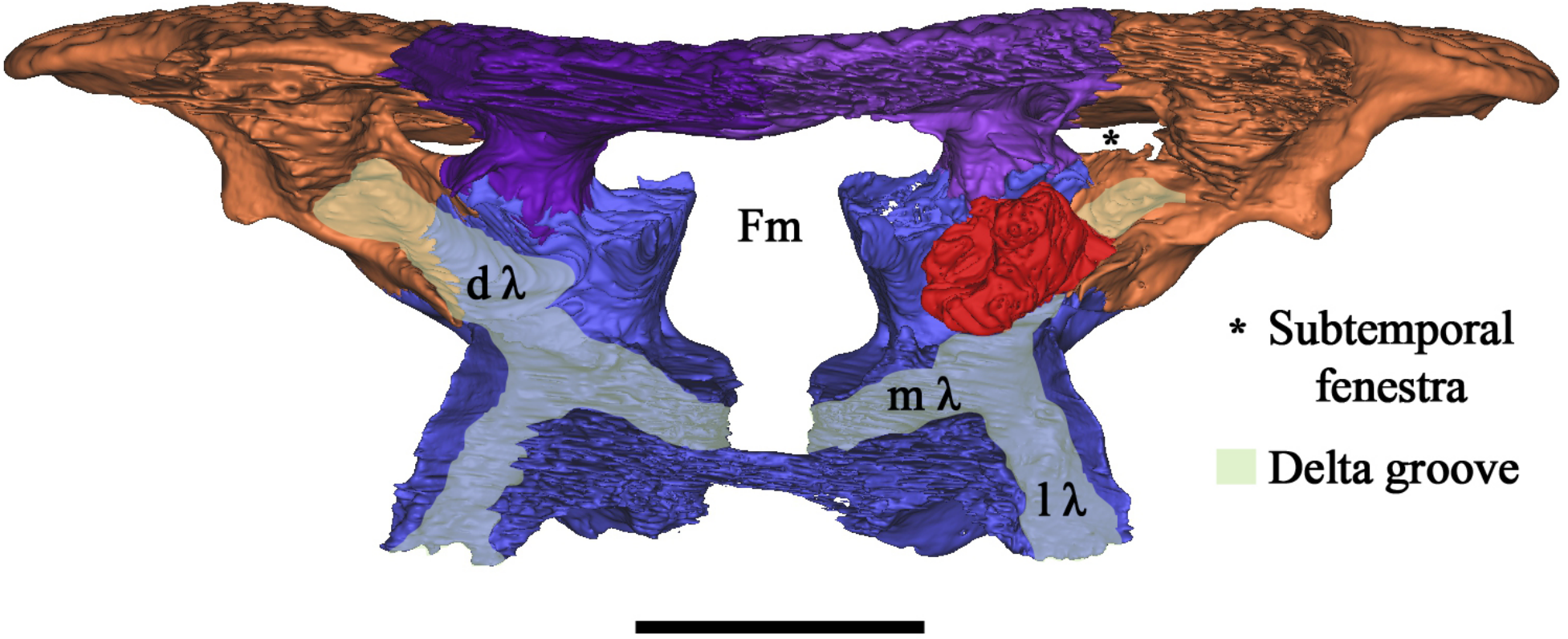
Fm
d λ
m λ
l λ
*
* Subtemporal fenestra
Delta groove

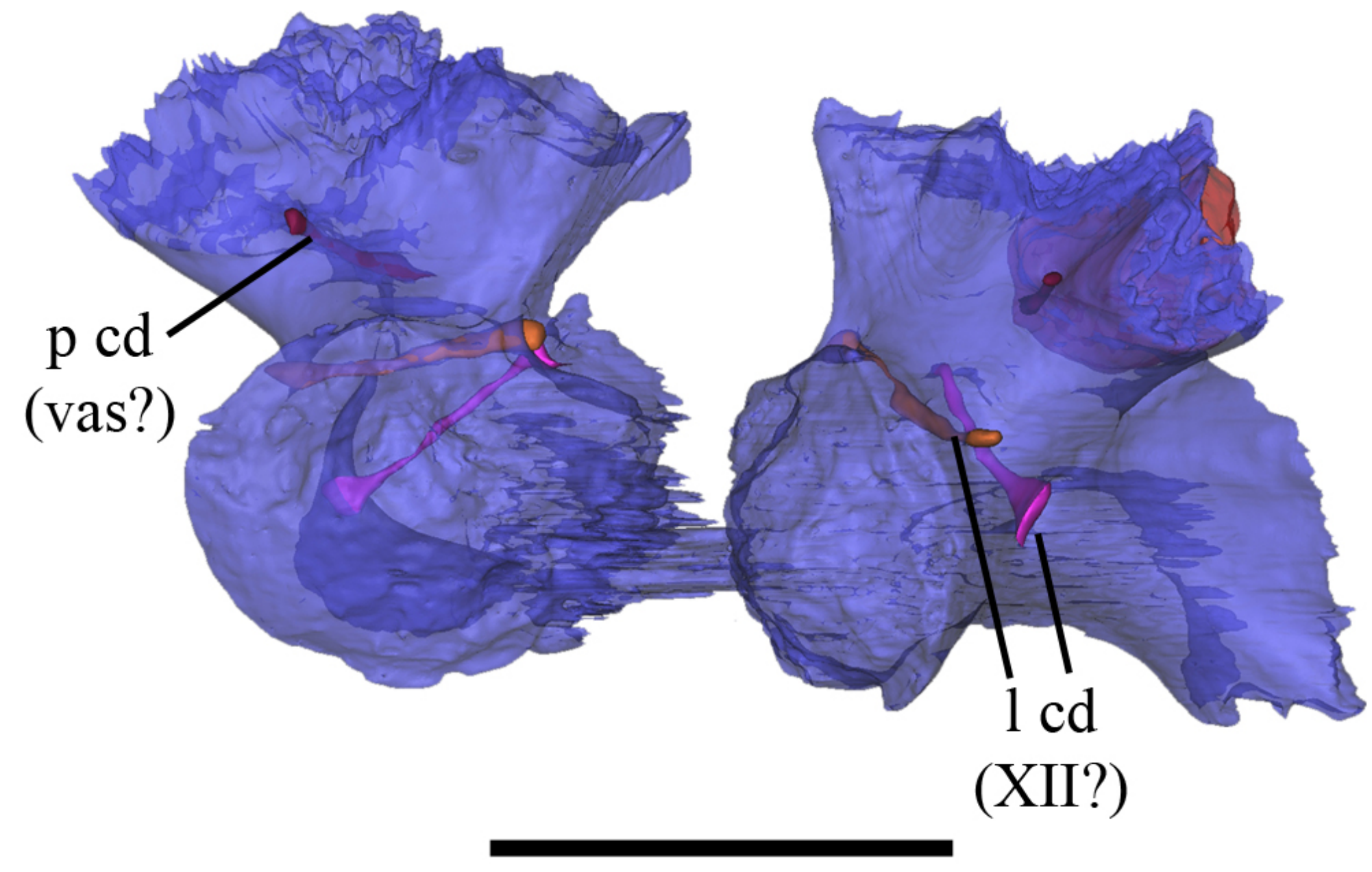
p cd
(vas?)
l cd
(XII?)

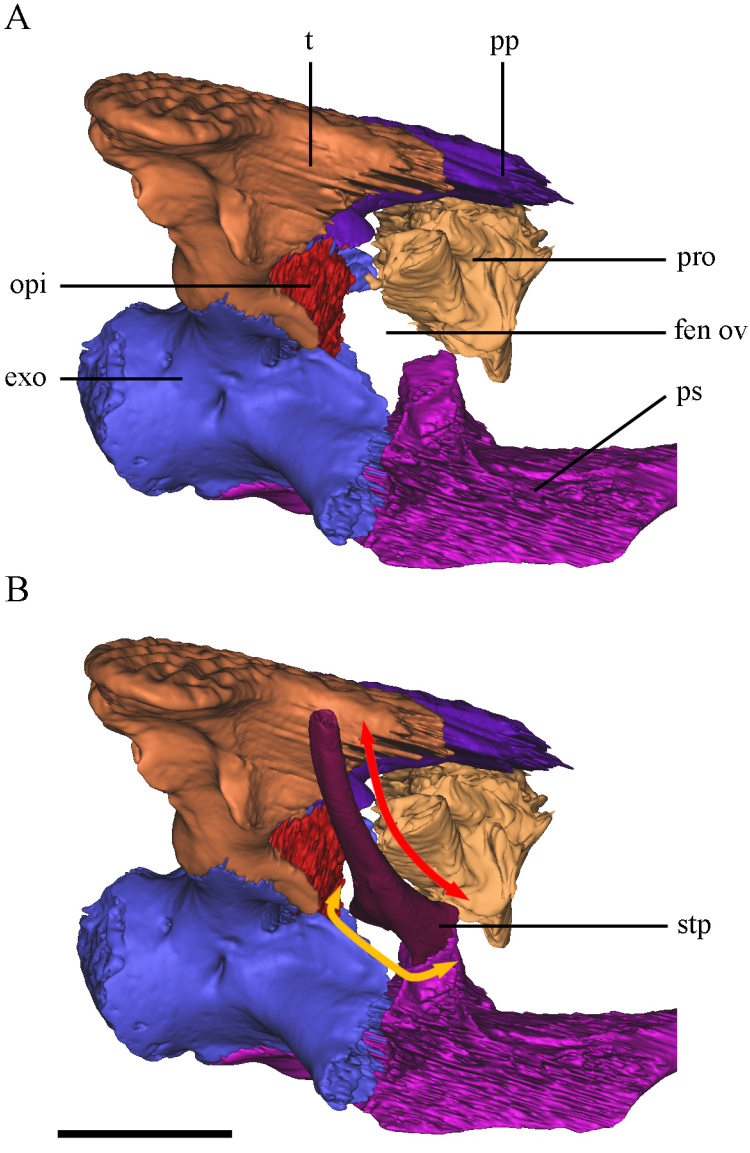
A
t
pp
pro
opi
fen ov
exo
ps
B
stp

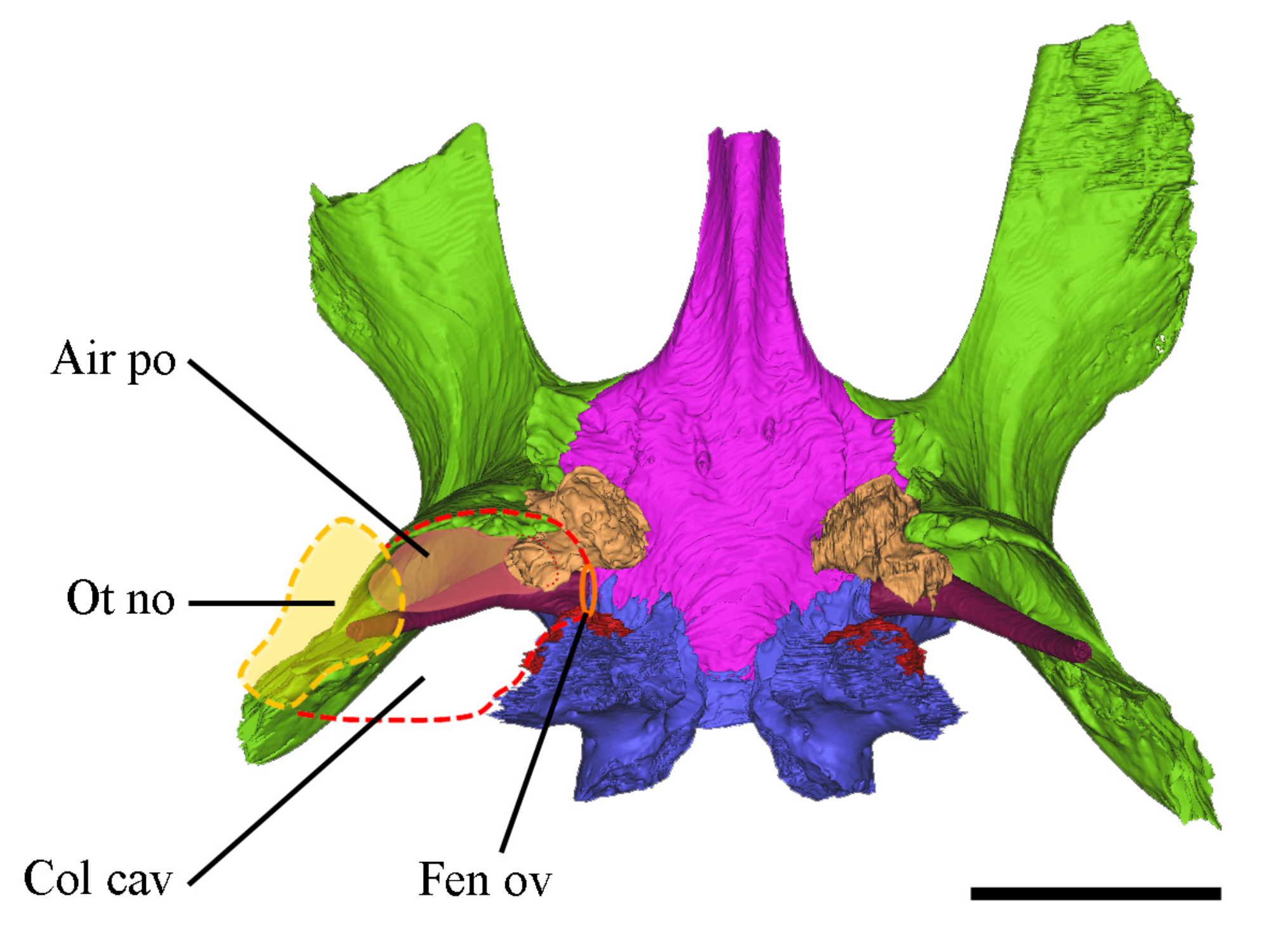
Air po
Ot no
Col cav
Fen ov